Robust Finite-Resolution Transceivers for Decentralized Estimation in Energy Harvesting Aided IoT Networks

Kunwar Pritiraj Rajput, *Member, IEEE,* Mohammad Faisal Ahmed, Naveen K. D. Venkategowda, *Senior Member, IEEE,* Aditya K. Jagannatham, *Senior Member, IEEE* and Lajos Hanzo, *Life Fellow, IEEE*

***Abstract*— This paper develop novel approaches for designing robust transceivers and energy covariance in an IoT network powered by energy harvesting. Our goal is to minimize the mean square error (MSE) at the fusion center (FC) while considering the uncertainty of channel state information (CSI). The proposed designs incorporate both Gaussian and bounded CSI uncertainty models to model the uncertainty in the CSI. Furthermore, two different optimal bit allocation scheme have been proposed for quantizing the measurements from each sensor node (SeN). However, solving the resulting MSE optimization problems with constraints on individual SeN power and total bit rate proves to be challenging due to their non-convex nature under both CSI uncertainty models. To address this challenge, we develop a block coordinate descent (BCD) based iterative framework. This framework leverages the block-convexity of the optimization objective and provides efficient solutions for both uncertainty paradigms considered. By making use of this analytical tractability, we obtain improved performance compared to the uncertainty-agnostic scheme that disregards CSI uncertainty. We validate our approach through numerical simulations, which not only support our analytical findings but also demonstrate the superior performance achieved with our method that accounts for CSI uncertainty.**

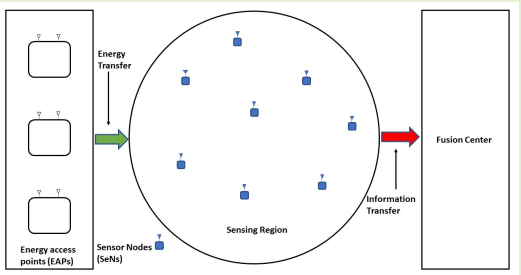

***Index Terms*— Bounded CSI uncertainty, decentralized estimation, Gaussian CSI uncertainty, Internet of Things, multiple access channel, parameter estimation, quantization, robust transceiver design.**

I. Introduction

Internet of Things networks (IoTNes) have extensive applications in sensing [1], monitoring [2], surveillance [3], etc., since they enable applications such as remote surveillance [4], industrial automation [5], smart agriculture [6], and healthcare [7]. However, IoTNes suffer from the limitation of a short lifetime as the sensor nodes (SeNs) depend on batteries that are either costly or even infeasible to replace/ recharge due to the harsh environment in which the SeNs are typically deployed. A promising solution is energy harvesting (EH)-IoTNes, where the SeNs harvest energy from the radio frequency (RF) signals transmitted by the energy access points (EAPs) and subsequently, utilize the acquired power for recording their observations and transmitting them to the fusion center (FC) [8].

In a typical linear decentralized setup [9], the IoTNe consists of a large number of SeNs that monitor the geographical area of interest and subsequently transmit their observations over a wireless channel to the FC. In order to overcome the performance loss arising due to the wireless fading channel between each SeN and the FC, and also to efficiently utilize the available power at the SeN, it is necessary to suitably process the SeN observations prior to their transmission. The SeNs transmit their pre-processed observations over a coherent multiple access channel (MAC) to the FC [9]–[12]. This requires determining the optimal transmit precoders (TPCs) at each SeN that minimize the mean square error (MSE). Moreover, it is equally important to optimally combine the received signals at the FC to minimize the MSE of parameter estimation. In addition, since a wireless powered IoTNe utilizes the energy harvested by the SeNs for its operation,

L. Hanzo would like to acknowledge the financial support of the Engineering and Physical Sciences Research Council projects EP/W016605/1, EP/X01228X/1 and EP/Y026721/1 as well as of the European Research Council's Advanced Fellow Grant QuantCom (Grant No. 789028). The work of Aditya K. Jagannatham was supported in part by the Qualcomm Innovation Fellowship, Qualcomm University Relations gift under the 6G UR India program, and in part by the Arun Kumar Chair Professorship.

K. P. Rajput was with the Department of Electrical Engineering, Indian Institute of Technology, Kanpur, Kanpur, 208016, India. He is now with the interdisciplinary center of security reliability and trust (SnT), University of Luxembourg, 1855, Luxembourg (e-mail: kunwar.rajput@uni.lu). M. F. Ahmed is with Cisco Systems India Pvt. Ltd., Bengaluru, India (e-mail: mdfaisal165@gmail.com). A. K. Jagannatham is with the Department of Electrical Engineering, Indian Institute of Technology, Kanpur, Kanpur, 208016, India (e-mail:adityaj@iitk.ac.in). N. K. D. Venkategowda is with the Department of Science and Technology, Linköping University, 60174 Norrköping, Sweden (e-mail: naveen.venkategowda@liu.se.). L. Hanzo is with the School of Electronics and Computer Science, University of Southampton, Southampton SO17 1BJ, U.K. (e-mail:lh@ecs.soton.ac.uk)

TABLE I
CONTRIBUTIONS OF THIS PAPER IN CONTRAST TO EXISTING LITERATURE

Feature	[12]	[14]	[15]	[170]	[18]	[19]	[20]	[21]	[225]	[24]	[26]	**Our work**
Energy Harvesting IoTNe		✓	✓	✓	✓	✓	✓	✓	✓	✓	✓	✓
Vector Parameter Estimation						✓	✓			✓		✓
Per SeN Power Constraint	✓	✓		✓	✓	✓	✓	✓	✓	✓	✓	✓
Coherent MAC	✓					✓	✓					✓
Joint Transceiver and Energy Covariance Matrices		✓				✓						✓
Quantized Transmission										✓	✓	✓
Gaussian CSI Uncertainty												✓
Bounded CSI Uncertainty												✓

one has to design the optimal energy covariance matrices for each EAP. Furthermore, due to the limited bandwidth available and to facilitate the error-resilient digital transmission of the SeN observations, there is a need to quantize them. Finally, in practice, perfect channel state information (CSI) cannot be guaranteed at either the FC or the SeNs. Therefore one also has to take the CSI uncertainty into account. Hence, for efficient estimation in EH-IoTNes, it is critically important to design robust joint transceivers and energy covariance matrices, so that the resultant MSE is minimized at the FC in the presence of CSI uncertainty, considering also quantized measurement transmissions. The state-of-the-art is presented next.

A. Review of existing contributions

Wireless energy transfer (WET) [13] technology has facilitated the development of EH-IoTNes, where, the SeNs harvest energy from the RF signals received from the EAPs in the first phase and in the second phase, the SeNs sense/monitor an event of interest and subsequently, transmit their observations to the FC for final estimation. Hence, researchers have focussed extensively on developing efficient techniques for energy harvesting and observation transmission in IoTNes [14], [15]. Zhou *et al.* [16] have proposed optimal estimation strategies under the deterministic and stochastic energy harvesting constraints with an objective to minimize the MSE at the FC. Guo *et al.* [17] have proposed an energy-efficient technique for sum throughput maximization in a clustered IoTNe, where the relay nodes are powered by the energy harvested from the RF signals transmitted by the SeNs. Xu *et al.* in [18] have developed an efficient SeN selection scheme considering the power required toward driving the circuit as well as for sensing or acquiring observations. Moreover, an interesting framework for joint energy and information beamforming has also been developed in their work for maximizing the signal-to-noise ratio (SNR) at the FC. Venkategowda *et al.* [19] conceives an alternating minimization based framework to determine the optimal power split between the sensing and data transmission operations. Venkategowda *et al.* [20] have also developed a novel decentralized and distributed transceiver design coupled with optimization of the energy covariance matrices for efficient vector parameter estimation. Knorn *et al.* [21] considered a IoTNe where the SeNs are battery operated and can also harvest energy. Interestingly, they can also share their energy with other "needy" SeNs in the IoTNe. An efficient estimation framework is developed for distortion minimization at the FC. Knorn *et al.* [22] also studied optimal power control for transmitting observations as well as sharing their energy with the "power-starved" SeNs for spatially correlated vector parameter estimation in an EH-IoTNe. The authors of [23] have conceived efficient unmanned ariel vehicle (UAV) trajectory design algorithm where UAV acts as remote charging device for the SeNs. Liu *et al.* [24] have recently proposed a novel scheme for joint node selection and beamforming toward transmit power minimization in an intelligent reflecting surface (IRS) assisted IoT network. The authors of [25] have developed an interesting joint transmit and reflective beamforming scheme for secure parameter estimation in the presence of an eavesdropper. The authors of [26] and [27] have exploited passive and active IRSs in an EH-IoTNe, wherein the IRSs aid in the energy harvesting as well as measurement transmission operations. However, they do not consider random parameter estimation in presence of observation noise and CSI uncertainty. Wang *et al.* [28] have studied an IRS-aided EH-IoT for random parameter estimation with single antenna IoT devices, assuming the availability of perfect CSI, which is impractical. Recently, the authors of [29] have proposed an unsupervised deep learning-based scheme toward spectral efficiency maximization in an industrial IoTNe. Cheng *et al.* proposed two different joint collaboration and compression designs for sequential estimation and detection in [30] and [31], respectively, of a random parameter in a wireless sensor network. Fang *et al.* [32] developed novel strategies based on two sleep scheduling policies with multiple vacations and start up thresholds for reduction of the peak age of information and power consumption reduction in an EH-IoTNe. However, it is important to note that all the above contributions rely on analog observation transmission, which would require an infinite number of bits, and are thus impractical. Therefore, quantization of the observations is desirable in a IoTNe, hence works related to this are reviewed next.

Battiloro *et al.* [33] have studied quantization in decentralized estimation of a time-varying parameter in a dynamically time-varying propagation environment. Zhan *et al.* [34] proposed a sub-optimal algorithm for the UAV trajectory design where UAV acts as a mobile FC and collects the quantized measurements from all the SeNs in an efficient way. Biswas *et al.* [35] developed an innovative optimal sensing and quantization rate allocation framework for detecting the change in the signal under observation with minimal delay. Sani and Vosoughi [36] proposed a two step procedure for

decentralized estimation subject to individual SeN and total bit-rate budget constraints. In the first step, the contributions of the observation and quantization noises as well as of channel fading are separated in the MSE function and then subsequently, both coupled and decoupled approaches are derived for solving the resultant optimization problem to achieve optimal resource allocation. Sani and Vosoughi in [37] also presented various strategies for quantizing the SeN observations affected by Gaussian additive and unknown multiplicative observation noise. However, both [36] and [37] considered an orthogonal MAC in their analysis, which is not bandwidth efficient [9]. A technique is conceived for spatial random field reconstruction in [38] by Nevat *et al.* subject to power and total bit rate constraints. Distributed estimation technique relying of probabilistic quantization which does not have to know the probability density function (PDF) is developed by Leung *et al.* [39]. Ciuonzo *et al.* [40] proposed a distributed detection scheme using the Rao test where the SeNs transmit their observation vectors using only a single bit or a few bits. A major limitation of these works is that they rely on the perfect CSI knowledge of all the SeN-FC links, which is an unrealistic assumption only. Very few authors have incorporated imperfect CSI in their analysis followed by the development of robust designs. These are reviewed next.

A novel rate distortion theory based optimal quantization scheme together with robust precoder design is proposed by Rajput *et al.* [41] for the estimation of a temporally correlated vector parameter using MSE minimization. Venakategowda *et al.* [42] proposed robust precoding schemes under bounded CSI uncertainty for scalar parameter estimation. However, the design described of [42] is based on the zero-forcing framework that results in noise enhancement at the FC. Zhu *et al.* [43] have developed a novel robust beamforming design for vector parameter estimation, once again for the bounded CSI uncertainty model. Along similar lines, Liu *et al.* [44] developed path-breaking linear robust transceiver designs for decentralized and distributed estimation as well as for total power minimization in the presence of CSI uncertainty. A novel algorithm is conceived for joint channel estimation and robust transceiver design in the context of sparse parameter estimation in [45] under Gaussian CSI uncertainty. The authors of [46] developed non-iterative robust transceiver designs for MSE minimization and quality of service constraint based designs considering Gaussian and norm ball CSI uncertainties. However, the works in [41]–[46] have not considered an EH-IoTNe in their analysis. In Table I we boldly and explicitly contrast novel contributions to the salient works in the open literature.

However, to the best of our knowledge, there is no literature related to EH-IoTNes proposing techniques for the design of robust transceivers and energy covariance matrices coupled with optimal bit allocation for the quantization of each SeN's observations under CSI uncertainty. Hence we intend to fill this knowledge gap. The next subsection elaborates on the salient contributions of this work in more depth.

B. Our contributions

The novel contributions of this paper are as follows.

- Initially, we derive the expression for the mean squared error (MSE) of a random parameter estimation by considering the Gaussian channel state information (CSI) uncertainty model [47]. We demonstrate that the problem of minimizing the resultant MSE is non-convex. Therefore, we propose an iterative framework based on block coordinate descent (BCD) to solve this problem. The framework determines the optimal bit allocation, robust receiver combiner (RC), TPCs and energy covariance matrices.
- We first derive a closed-form expression for the optimal quantization of the observation vector. Subsequently, we derive a robust RC that minimizes the parameter estimation MSE. Finally, we formulate the TPC and energy covariance matrices design problem as a quadratically constrained quadratic program (QCQP), which can be solved using a suitable convex optimization tool.
- To provide a more comprehensive analysis, we extend the optimal bit allocation, energy covariance matrices and robust transceiver design to the bounded CSI uncertainty model [48]. We again employ the BCD-based iterative framework and solve two different epigraph-based optimization problems iteratively. This approach allows us to obtain the optimal bit allocation vector, energy covariance matrices and robust transceivers.
- Finally, through simulation results, we demonstrate the effectiveness of the proposed schemes and their superior performance compared to the agnostic design that ignores the CSI uncertainty.

The rest of the manuscript is organized as follows. Section-II presents the system model of energy harvesting, sensing and estimation of the parameter vector. Section-III develops the framework for optimal bit allocation followed by our joint robust transceiver design relying on average MSE minimization at the FC under Gaussian CSI uncertainty. Section-IV develops our quantization and robust transceiver design for worst-case MSE minimization under bounded CSI uncertainty. Our simulation results are discussed in Section-V, while Section-VI provides our conclusion.

Notation: The notation $\mathbf{x} \sim \mathcal{N}(\mathbf{0}, \mathbf{R}_x)$, for an n dimensional real vector $\mathbf{x}$, denotes that it follows the Gaussian distribution with mean $\mathbf{0}$ and covariance matrix $\mathbf{R}_x \in \mathbb{R}^{n\times n}$. $\mathbf{I}_n$ denotes an identity matrix of size $n \times n$, while $\mathbf{1}_{n\times m}$ denotes a $n \times m$ matrix whose each element is equal to one. $||\mathbf{x}||_2$ denotes the Euclidean norm of the vector quantity $\mathbf{x}$, whereas $||\mathbf{X}||_F$ represents the Frobenius norm of the matrix $\mathbf{X}$. Tr[.] and $\mathbb{E}$[.] denote the trace and statistical expectation operators, respectively. Furthermore, $\mathbf{X} = \text{diag}\,[x_1, x_2, \ldots, x_K]$ denotes a diagonal matrix with elements x_i for $i = 1, 2, \ldots, K$ on its principal diagonal. The operation $\mathbf{a} = \text{vec}(\mathbf{A})$ stacks the columns of the $m \times n$ matrix $\mathbf{A}$ to form a column vector $\mathbf{a}$ of dimension mn, whereas the operation $\text{vec}_n^{-1}(\mathbf{a})$ yields the matrix $\mathbf{A}$ having n columns and an appropriate number of rows.

II. System Model

As seen in Fig. 1, we consider an EH-IoTNe having K SeNs each equipped with N_t antennas, J-EAPs with N_j antennas

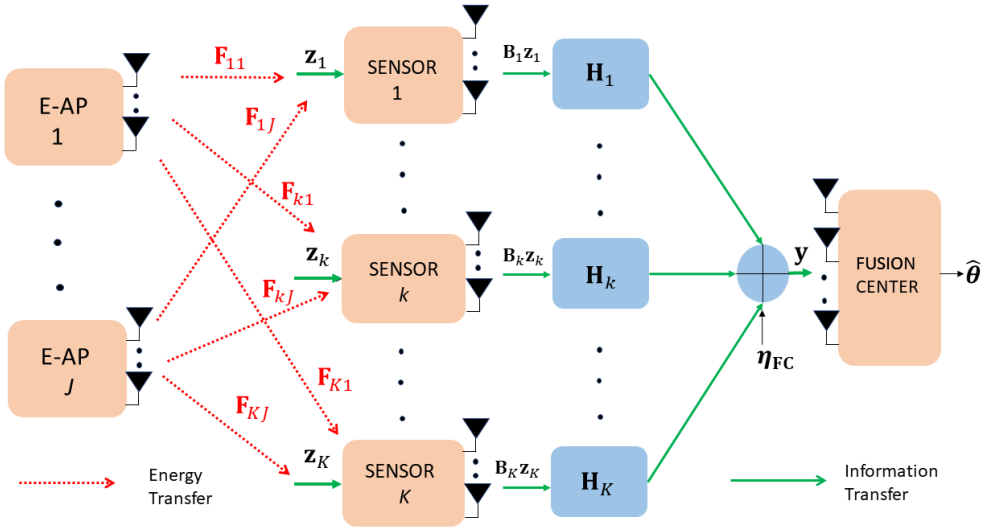

Fig. 1. System model for energy harvesting, parameter sensing and estimation in an EH-IoTNe.

installed at each EAP, and a FC equipped with N_r antennas. In this EH-IoTNe, the SeNs are powered by the energy harvested from the radio frequency (RF) signals transmitted by the EAPs. Toward this end, during the WET phase, the signal transmitted by the jth EAP is denoted by $\mathbf{x}_j \in \mathbb{R}^{N_j \times 1}$ with its covariance matrix represented by $\mathbf{\Phi}_j \in \mathbb{R}^{N_j \times N_j}$. The power transmitted from the jth EAP is constrained as $\mathrm{Tr}\left[\mathbf{\Phi}_j\right] \leq \gamma_{T,j}$, for $j = 1, 2, \ldots, J$, where $\gamma_{T,j}$ represents the total transmit power budget of the jth EAP. Next, defining the channel between the jth EAP and the kth SeN as $\mathbf{F}_{kj} \in \mathbb{R}^{N_t \times N_j}$, the expression for the total harvested power of the kth SeN, denoted by $\gamma_{h,k}$, can be formulated as

$$\gamma_{h,k} = \zeta_k \mathbb{E}\left[\left\| \sum_{j=1}^{J} \mathbf{F}_{kj}\mathbf{x}_j \right\|_F^2\right] = \zeta_k \sum_{j=1}^{J} \mathrm{Tr}\left[\mathbf{F}_{kj}\mathbf{\Phi}_j\mathbf{F}_{kj}^H\right], \tag{1}$$

where $0 < \zeta_k \leq 1$, represents the energy harvesting efficiency of the kth SeN.

The observation vector $\mathbf{z}_k \in \mathbb{R}^{l_k \times 1}$ corresponding to the kth SeN is modelled as

$$\mathbf{z}_k = \mathbf{D}_k\boldsymbol{\theta} + \boldsymbol{\eta}_k, \tag{2}$$

where $\mathbf{D}_k \in \mathbb{R}^{l_k \times m}$ and $\boldsymbol{\eta}_k \sim \mathcal{N}(\mathbf{0}, \mathbf{\Psi}_k) \in \mathbb{R}^{l_k \times 1}$ denote the observation matrix and noise vector, respectively, corresponding to the kth SeN. The unknown parameter vector to be estimated is denoted by $\boldsymbol{\theta} \in \mathbb{R}^{m \times 1}$ and is assumed to be distributed as $\mathcal{N}(\mathbf{0}, \mathbf{\Sigma}_\theta)$. The dynamic sensing range of each SeN is considered to lie in the closed interval $[-W, W]$ [36], [49]. The lth element of the observation vector $\mathbf{z}_k$ is denoted by $z_{l,k} \in \mathbb{R}$, and is to be quantized using $\beta_{l,k}$ bits. The corresponding step size $\Delta_{l,k}$ is mathematically represented as

$$\Delta_{l,k} = \frac{2W}{2^{\beta_{l,k}} - 1}. \tag{3}$$

Furthermore, the corresponding quantization noise will be uniformly distributed with its variance denoted by $\frac{(\Delta_{l,k})^2}{12}$, which can be expressed as [36]

$$\frac{(\Delta_{l,k})^2}{12} = \frac{W^2}{3\left(2^{\beta_{l,k}} - 1\right)^2} \approx \frac{W^2}{3\left(2^{\beta_{l,k}}\right)^2}. \tag{4}$$

Since, $z_{l,k}$ is quantized using $\beta_{l,k}$ bits, the number of quantization levels is equal to $2^{\beta_{l,k}}$. The corresponding quantized output $z_{l,k}^q$ takes values from the set $\mathcal{Z}_{l,k}$ defined as

$$\mathcal{Z}_{l,k} \in \left\{z_{l,k,1}^q, z_{l,k,2}^q, \ldots, z_{l,k,2^{\beta_{l,k}}}^q\right\}, \tag{5}$$

where $z_{l,k,n}^q$ is defined as

$$z_{l,k,n}^q = \frac{\left(2n - 1 - 2^{\beta_{l,k}}\right)\Delta_{l,k}}{2}, \tag{6}$$

where $n = 1, 2, \ldots, 2^{\beta_{l,k}}$. If $z_{l,k} \in \left[z_{l,k,n}^q - \frac{\Delta_{l,k}}{2}, z_{l,k,n}^q + \frac{\Delta_{l,k}}{2}\right]$ then $z_{l,k}^q = z_{l,k,n}^q$. Hence, the quantized output $z_{l,k}^q$ follows:

$$z_{l,k}^q = \begin{cases} W & \text{if } z_{l,k} \geq W \\ z_{l,k,n}^q \in \mathcal{Z}_{l,k} & \text{if } -W < z_{l,k,n}^q - \frac{\Delta_{l,k}}{2} < z_{l,k} \\ & \quad < z_{l,k,n}^q + \frac{\Delta_{l,k}}{2} < W \\ -W & \text{if } z_{l,k} \leq -W. \end{cases} \tag{7}$$

The quantized counterpart of the observation vector $\mathbf{z}_k$ in (2), denoted by $\mathbf{z}_k^q$, can be mathematically modeled as

$$\mathbf{z}_k^q = \mathbf{D}_k\boldsymbol{\theta} + \boldsymbol{\eta}_k + \boldsymbol{\eta}_k^q = \mathbf{D}_k\boldsymbol{\theta} + \boldsymbol{\eta}_k^e. \tag{8}$$

The quantity $\boldsymbol{\eta}_k^q \in \mathbb{R}^{l_k \times 1}$ denotes the ensuing quantization noise which is uniformly distributed with zero mean and covariance matrix $\mathbf{\Psi}_k^q \in \mathbb{R}^{l_k \times l_k}$, that is represented as

$$\mathbf{\Psi}_k^q = \mathrm{diag}\left[\frac{W^2}{3\left(2^{\beta_{1,k}}\right)^2}, \frac{W^2}{3\left(2^{\beta_{2,k}}\right)^2}, \ldots, \frac{W^2}{3\left(2^{\beta_{l,k}}\right)^2}\right]. \tag{9}$$

Furthermore, the quantization noise $\boldsymbol{\eta}_k^q \in \mathbb{R}^{l_k \times 1}$ is uncorrelated with $\boldsymbol{\eta}_k$ [50]. The quantity $\boldsymbol{\eta}_k^e = \boldsymbol{\eta}_k + \boldsymbol{\eta}_k^q$ denotes the effective noise after quantization which has a covariance

matrix, given by $\mathbf{\Psi}_k^e = \mathbf{\Psi}_k + \mathbf{\Psi}_k^q \in \mathbb{R}^{l_k \times l_k}$. Let us assume that the total bit-rate budget to quantize each SeN's observation is $\mathcal{B}$ bits. This implies that the following constraint should be satisfied:

$$\sum_{k=1}^{K}\sum_{l=1}^{l_k} \beta_{l,k} = \mathbf{1}^T \boldsymbol{\beta} \leq \mathcal{B}, \tag{10}$$

where the quantity $\boldsymbol{\beta} \in \mathbb{R}^{Kl\times 1}$ is defined as $\boldsymbol{\beta} = [\beta_{1,1}, \beta_{2,1}, \ldots, \beta_{l_K,K}]^T$ and $l = \sum_{k=1}^{K} l_k$.

In order to combat the adverse effects of fading in the channel between each SeN and the FC and due to the transmit power limitation at each SeN in the EH-IoTNe, it is necessary for each SeN to pre-processes its observation vector using the TPC matrix $\mathbf{B}_k \in \mathbb{R}^{N_t \times l_k}$. Subsequently, each SeN transmits the precoded observation over a coherent MAC to the FC for receive combining. The vector $\mathbf{y} \in \mathbb{R}^{N_r \times 1}$ received at the FC is given by

$$\mathbf{y} = \sum_{k=1}^{K} \mathbf{H}_k \mathbf{B}_k \mathbf{D}_k \boldsymbol{\theta} + \sum_{k=1}^{K} \mathbf{H}_k \mathbf{B}_k \boldsymbol{\eta}_k^e + \boldsymbol{\eta}_{\mathrm{FC}}, \tag{11}$$

where $\mathbf{H}_k \in \mathbb{R}^{N_r \times N_t}$ denotes the wireless fading MIMO channel matrix between the kth SeN and the FC, while the vector $\boldsymbol{\eta}_{\mathrm{FC}} \sim \mathcal{CN}(\mathbf{0}, \mathbf{\Psi}_{\mathrm{FC}}) \in \mathbb{R}^{N_r \times 1}$ represents the FC noise. Subsequently, at the FC, the RC matrix $\mathbf{A} \in \mathbb{R}^{N_r \times m}$ is used to produce the estimate $\widehat{\boldsymbol{\theta}} = \mathbf{A}^H \mathbf{y}$ of the unknown parameter vector of interest $\boldsymbol{\theta}$ as

$$\widehat{\boldsymbol{\theta}} = \sum_{k=1}^{K} \mathbf{A}^H \mathbf{H}_k \mathbf{B}_k \mathbf{D}_k \boldsymbol{\theta} + \sum_{k=1}^{K} \mathbf{A}^H \mathbf{H}_k \mathbf{B}_k \boldsymbol{\eta}_k^e + \mathbf{A}^H \boldsymbol{\eta}_{\mathrm{FC}}. \tag{12}$$

The resultant $\mathrm{MSE} = \mathrm{Tr}\left[\mathbb{E}\left[\left(\widehat{\boldsymbol{\theta}} - \boldsymbol{\theta}\right)\left(\widehat{\boldsymbol{\theta}} - \boldsymbol{\theta}\right)^H\right]\right]$ can be expressed as

$$\begin{aligned}\mathrm{MSE} = \mathrm{Tr}\Bigg[&\mathbf{A}^H \left(\sum_{k=1}^{K} \mathbf{H}_k \mathbf{B}_k \mathbf{D}_k\right) \mathbf{\Sigma}_\theta \left(\sum_{k=1}^{K} \mathbf{H}_k \mathbf{B}_k \mathbf{D}_k\right)^H \mathbf{A} \\ &+ \mathbf{A}^H \sum_{k=1}^{K} \mathbf{H}_k \mathbf{B}_k \mathbf{\Psi}_k^e \mathbf{B}_k^H \mathbf{H}_k^H \mathbf{A} + \mathbf{A}^H \mathbf{\Psi}_{\mathrm{FC}} \mathbf{A} + \mathbf{\Sigma}_\theta \\ &- \mathbf{A}^H \sum_{k=1}^{K} \mathbf{H}_k \mathbf{B}_k \mathbf{D}_k \mathbf{\Sigma}_\theta - \left(\mathbf{A}^H \sum_{k=1}^{K} \mathbf{H}_k \mathbf{B}_k \mathbf{D}_k \mathbf{\Sigma}_\theta\right)^H\Bigg].\end{aligned} \tag{13}$$

The transmit power constraint of the kth SeN is given as follows

$$\begin{aligned}&t\gamma_{c,k} + t_I \mathbb{E}\left[\|\mathbf{B}_k \mathbf{z}_k^q\|_2^2\right] \\ &= t\gamma_{c,k} + t_I \mathrm{Tr}\left[\mathbf{B}_k \left(\mathbf{D}_k \mathbf{\Sigma}_\theta \mathbf{D}_k^H + \mathbf{\Psi}_k^e\right) \mathbf{B}_k^H\right] \leq t_E \gamma_{h,k},\end{aligned} \tag{14}$$

where the quantities $\gamma_{c,k}$, t_I and t_E represent the power consumption in the circuit, time duration of information transmission and time duration of energy harvesting, respectively. The total time duration is given by $t = t_I + t_E$. The next section develops an iterative framework for optimal bit allocation to quantize each SeN's observations optimally for a given bit-rate budget, robust transceiver and energy covariance matrices design considering Gaussian CSI uncertainty.

III. Quantization and Robust Transceiver Design under Gaussian CSI Uncertainty

Due to several restrictions, such as the limited pilot overhead, quantization error, feedback latency, and so on, in practice it is typically not possible to get perfect information about the underlying channels between each SeN and the FC. Hence, there is a pressing need to design resilient transceivers that account for CSI uncertainty in order to offset the performance loss caused by imperfect channel state information (CSI). In such a scenario, the true channel $\mathbf{H}_k$ between each SeN k and the FC, can be represented as

$$\mathbf{H}_k = \widehat{\mathbf{H}}_k + \Delta\mathbf{H}_k, \tag{15}$$

where $\widehat{\mathbf{H}}_k$ denotes the available estimate and $\Delta\mathbf{H}_k$ represents the estimation error matrix. In the Gaussian CSI uncertainty framework, each element of $\Delta\mathbf{H}_k$ is considered to be distributed as $\mathcal{CN}\left(0, \sigma_H^2\right)$, where σ_H^2 is termed the uncertainty variance. The following lemma is used to derive the expression of the average MSE from the MSE expression given in (13).

Lemma 1: Consider the matrix $\mathbf{G} \in \mathbb{R}^{N_r \times N_t}$, represented as $\mathbf{G} = \widehat{\mathbf{G}} + \Delta\mathbf{G}$, where the matrix $\widehat{\mathbf{G}}$ is the available CSI estimate and the elements of the matrix $\Delta\mathbf{G}$ are independent and identically distributed Gaussian random variables with mean 0 and variance σ_G^2. Then for any matrix $\mathbf{E}$ of appropriate dimension, the following results hold

$$\begin{aligned}&\mathbb{E}_{\Delta\mathbf{G}}\left[\mathbf{G}\mathbf{E}\mathbf{E}^H\mathbf{G}^H\right] = \widehat{\mathbf{G}}\mathbf{E}\mathbf{E}^H\widehat{\mathbf{G}}^H + \sigma_G^2 \mathrm{Tr}\left[\mathbf{E}\mathbf{E}^H\right]\mathbf{I}_{N_r}, \\ &\mathbb{E}_{\Delta\mathbf{G}}\left[\widehat{\mathbf{G}}\mathbf{E}\mathbf{E}^H\Delta\mathbf{G}^H\right] = \mathbb{E}_{\Delta\mathbf{G}}\left[\Delta\mathbf{G}\mathbf{E}\mathbf{E}^H\widehat{\mathbf{G}}^H\right] = \mathbf{0}.\end{aligned} \tag{16}$$

Substituting the true channel $\mathbf{H}_k$ according to (15) in the MSE expression in (13), and further employing the results given in Lemma 1, one obtains the expression for the average MSE as

$$\begin{aligned}\overline{\mathrm{MSE}} = &\mathrm{Tr}\left[\mathbf{A}^H \left(\sum_{k=1}^{K} \widehat{\mathbf{H}}_k \mathbf{B}_k \mathbf{D}_k\right) \mathbf{\Sigma}_\theta \left(\sum_{k=1}^{K} \widehat{\mathbf{H}}_k \mathbf{B}_k \mathbf{D}_k\right)^H \mathbf{A}\right] \\ &+ \mathrm{Tr}\Big[\mathbf{A}^H \sigma_H^2 \mathrm{Tr}\Big[\sum_{k=1}^{K} \mathbf{B}_k \left(\mathbf{D}_k \mathbf{\Sigma}_\theta \mathbf{D}_k^H + \mathbf{\Psi}_k\right) \mathbf{B}_k^H\Big] \mathbf{A}\Big] \\ &- 2\mathrm{Tr}\left[\mathbf{A}^H \sum_{k=1}^{K} \widehat{\mathbf{H}}_k \mathbf{B}_k \mathbf{D}_k \mathbf{\Sigma}_\theta\right] + \mathrm{Tr}\left[\mathbf{\Sigma}_\theta\right] + \mathrm{Tr}\left[\mathbf{A}^H \mathbf{\Psi}_{\mathrm{FC}} \mathbf{A}\right] \\ &+ \mathrm{Tr}\left[\mathbf{A}^H \sum_{k=1}^{K} \widehat{\mathbf{H}}_k \mathbf{B}_k \mathbf{\Psi}_k \mathbf{B}_k^H \widehat{\mathbf{H}}_k^H \mathbf{A}\right].\end{aligned} \tag{17}$$

The energy covariance matrices $\mathbf{\Phi}_j$, $\forall\ j$, are simultaneously determined to improve the harvested energy. The challenge of designing the ideal transceiver that minimises the MSE in (17) while respecting the individual SeN power limitation in (14) and the total bit-rate constraint, can be formulated as

$$\begin{aligned}\underset{\mathbf{A}, \{\mathbf{B}_k\}_{k=1}^K, \{\mathbf{\Phi}_j\}_{j=1}^J, \boldsymbol{\beta}}{\text{minimize}} \quad & \overline{\mathrm{MSE}} \\ \text{subject to} \quad & t\gamma_{c,k} + t_I \mathrm{Tr}\left[\mathbf{B}_k \left(\mathbf{D}_k \mathbf{\Sigma}_\theta \mathbf{D}_k^H + \mathbf{\Psi}_k^e\right) \mathbf{B}_k^H\right] \\ & \leq t_E \gamma_{h,k},\ k = 1, 2, \ldots, K, \\ & \mathbf{1}^T \boldsymbol{\beta} \leq \mathcal{B} \\ & \mathrm{Tr}\left[\mathbf{\Phi}_j\right] \leq \gamma_{T,j}, \text{and } \mathbf{\Phi}_j \succeq \mathbf{0},\ \forall j.\end{aligned} \tag{18}$$

The optimization problem in (18) is non-convex, since the objective is non-convex in terms of the optimization variables $\mathbf{A}$, $\{\mathbf{B}_k\}_{k=1}^K$, $\{\mathbf{\Phi}_j\}_{j=1}^J$, $\boldsymbol{\beta}$ which renders it intractable. In order to handle the non-convexity of the optimization objective in (18), the block coordinate descent (BCD)-based alternating minimization framework that exploits the block convex nature of the optimization problem in (18) can be invoked. Hence, a BCD-based iterative framework is employed next to find the optimal bit allocation for the quantization of the SeNs' observations, followed by designing robust transceivers and energy covariance matrices that minimize the resultant MSE at the FC. The procedure of optimal bit allocation is described next in detail.

A. Optimal quantization of SeN observations for the Gaussian CSI uncertainty scenario

This subsection takes the limited bandwidth nature of the IoTNe into consideration and develops a scheme for optimally allocating the available bit-rate budget among the SeNs for quantizing the SeN observations. Substituting $\mathbf{\Psi}_k^e = \mathbf{\Psi}_k + \mathbf{\Psi}_k^q$ into the MSE expression of (17) and extracting the terms that depend only on the quantization noise covariance matrix $\mathbf{\Psi}_k^q$ for each SeN k, one can observe that only the terms $\mathrm{Tr}\left[\mathbf{A}^H \sum_{k=1}^K \widehat{\mathbf{H}}_k \mathbf{B}_k \mathbf{\Psi}_k^q \mathbf{B}_k^H \widehat{\mathbf{H}}_k^H \mathbf{A}\right]$ and $\mathrm{Tr}\left[\mathbf{A}^H \sigma_H^2 \mathrm{Tr}\left[\sum_{k=1}^K \mathbf{B}_k \mathbf{\Psi}_k^q \mathbf{B}_k^H\right] \mathbf{A}\right]$ depend on the quantization noise. Exploiting the property $\mathrm{Tr}(\mathbf{P}^H\mathbf{Q}\mathbf{P}\mathbf{R}) = \mathrm{vec}(\mathbf{P})^H \left(\mathbf{R}^T \otimes \mathbf{Q}\right) \mathrm{vec}(\mathbf{P})$, these terms can be recast as

$$\begin{aligned}&\mathrm{Tr}\left[\mathbf{A}^H \sum_{k=1}^K \widehat{\mathbf{H}}_k \mathbf{B}_k \mathbf{\Psi}_k^q \mathbf{B}_k^H \widehat{\mathbf{H}}_k^H \mathbf{A}\right] \\ &= \sum_{k=1}^K \mathrm{Tr}\left[\mathbf{A}^H \widehat{\mathbf{H}}_k \mathbf{B}_k \mathbf{\Psi}_k^q \mathbf{B}_k^H \widehat{\mathbf{H}}_k^H \mathbf{A}\right] = \sum_{k=1}^K \tilde{\mathbf{a}}_k^T \tilde{\mathbf{x}}_k, \end{aligned} \tag{19}$$

$$\begin{aligned}&\mathrm{Tr}\left[\mathbf{A}^H \sigma_H^2 \mathrm{Tr}\left[\sum_{k=1}^K \mathbf{B}_k \mathbf{\Psi}_k^q \mathbf{B}_k^H\right] \mathbf{A}\right] \\ &= \kappa \sum_{k=1}^K \mathrm{Tr}\left[\mathbf{B}_k \mathbf{\Psi}_k^q \mathbf{B}_k^H\right] = \sum_{k=1}^K \bar{\mathbf{a}}_k^T \tilde{\mathbf{x}}_k, \end{aligned} \tag{20}$$

where $\kappa = \sigma_H^2 \mathrm{Tr}\left[\mathbf{A}^H \mathbf{A}\right]$ and the vector quantities $\tilde{\mathbf{a}}_k^T \in \mathbb{R}^{1 \times l_k^2}$, $\bar{\mathbf{a}}_k^T \in \mathbb{R}^{1 \times l_k^2}$, $\tilde{\mathbf{x}}_k \in \mathbb{R}^{l_k^2 \times 1}$ are defined as

$$\tilde{\mathbf{a}}_k = \left[\left(\mathbf{B}_k^H \widehat{\mathbf{H}}_k^H \mathbf{A}\right)^T \otimes \mathbf{A}^H \widehat{\mathbf{H}}_k \mathbf{B}_k\right]^T \mathrm{vec}\left[\mathbf{I}_m\right] \tag{21}$$

$$\bar{\mathbf{a}}_k = \left[\left(\mathbf{B}_k^H\right)^T \otimes \mathbf{B}_k\right]^T \mathrm{vec}\left[\mathbf{I}_m\right] \tag{22}$$

$$\tilde{\mathbf{x}}_k = \mathrm{vec}\left[\mathbf{\Psi}_k^q\right]. \tag{23}$$

Since most of the entries of the vector $\tilde{\mathbf{x}}_k$ are zero, we define a new vector $\mathbf{x}_k$ that is derived by extracting the non-zero values of $\tilde{\mathbf{x}}_k$. Subsequently, the elements corresponding to the indices of the non-zero entries of $\tilde{\mathbf{x}}_k$ are extracted from both the vectors $\tilde{\mathbf{a}}_k$ as well as $\bar{\mathbf{a}}_k$ and then added together to obtain the vector $\mathbf{a}_k$. Therefore, the expressions in (19) and (20) can be equivalently written as

$$\sum_{k=1}^K \left(\tilde{\mathbf{a}}_k^T + \bar{\mathbf{a}}_k^T\right) \tilde{\mathbf{x}}_k = \sum_{k=1}^K \mathbf{a}_k^T \mathbf{x}_k = \mathbf{a}^T \mathbf{x}, \tag{24}$$

where we have $\mathbf{a} = [\mathbf{a}_1^T, \mathbf{a}_2^T, \ldots, \mathbf{a}_K^T]^T \in \mathbb{R}^{KL \times 1}$ and $L = \sum_{k=1}^K l_k^2$. Furthermore, the structure of the vector $\mathbf{x}_k \in \mathbb{R}^{KL \times 1}$ is given as

$$\mathbf{x}_k = \left[\frac{W^2}{3} 4^{-\beta_{1,k}}, \frac{W^2}{3} 4^{-\beta_{2,k}}, \ldots, \frac{W^2}{3} 4^{-\beta_{l_k,k}}\right], \tag{25}$$

for $1 \leq k \leq K$. The expression in (24) can be further simplified as

$$\mathbf{a}^T \mathbf{x} = \frac{W^2}{3} \mathbf{a}^T 4^{-\boldsymbol{\beta}}. \tag{26}$$

Hence, the optimization problem that minimizes the MSE derived in (26) above, subject to the total bit budget, can be readily formulated as

$$\begin{aligned} \underset{\boldsymbol{\beta}}{\text{minimize}} \quad & \frac{W^2}{3} \mathbf{a}^T 4^{-\boldsymbol{\beta}} \\ \text{subject to} \quad & \mathbf{1}^T \boldsymbol{\beta} \leq \mathcal{B}. \end{aligned} \tag{27}$$

The above optimization problem is convex in nature. As a result, to solve the aforementioned optimization problem, one can use the Karush-Kuhn-Tucker (KKT) framework [51], and the closed-form solution for the optimal bit allocation variable $\beta_{l,k}$ can be derived as

$$\begin{aligned}\beta_{l,k} = \frac{\mathcal{B}}{Kl} - \frac{1}{\ln(4)} \Bigg[\Bigg[\frac{1}{Kl} \sum_{i=1}^{Kl} \ln\left(\frac{a_{l,k} W^2}{3} \ln(4)\right) \Bigg] \\ - \ln(a_{l,k} \ln(4)) \Bigg]. \end{aligned} \tag{28}$$

The next subsection describes the procedure for deriving the optimal RC matrix with quantized SeN observations.

B. Receiver Combiner design

Using the quantized SeN observations and assuming the TPCs $\{\mathbf{B}_k\}_{k=1}^K$ to be known, the optimization problem of designing the ideal RC matrix $\mathbf{A}$ minimising the average MSE in (17) is an unconstrained quadratic optimization problem. As a result, the optimal RC matrix is obtained by differentiating the average MSE expression in (17) with respect to the RC matrix $\mathbf{A}$ and equating it to zero, where we have

$$\begin{aligned}\mathbf{A} = &\left[\left(\sum_{k=1}^K \widehat{\mathbf{H}}_k \mathbf{B}_k \mathbf{D}_k\right) \mathbf{\Sigma}_\theta \left(\sum_{k=1}^K \widehat{\mathbf{H}}_k \mathbf{B}_k \mathbf{D}_k\right)^H + \mathbf{\Psi}_{\mathrm{FC}} + \sigma_H^2 \right. \\ &\sum_{k=1}^K \mathrm{Tr}\left[\mathbf{B}_k \mathbf{D}_k \mathbf{\Sigma}_\theta \mathbf{D}_k^H \mathbf{B}_k^H\right] \mathbf{I}_{N_r} + \sum_{k=1}^K \widehat{\mathbf{H}}_k \mathbf{B}_k \mathbf{\Psi}_k^e \mathbf{B}_k^H \widehat{\mathbf{H}}_k^H \\ &\left. + \sigma_H^2 \sum_{k=1}^K \mathrm{Tr}\left[\mathbf{B}_k \mathbf{\Psi}_k^e \mathbf{B}_k^H\right] \mathbf{I}_{N_r}\right]^{-1} \sum_{k=1}^K \widehat{\mathbf{H}}_k \mathbf{B}_k \mathbf{D}_k \mathbf{\Sigma}_\theta. \end{aligned} \tag{29}$$

To obtain the optimal TPC matrices for a known RC matrix $\mathbf{A}$ with quantized SeN observations, one can modify the optimization objective in (18) and formulate a new optimization

problem in terms of the optimal TPC and energy covariance matrices, as described next in detail.

C. Transmit Precoder design

Upon defining the vector quantity $\mathbf{b}_k = \mathrm{vec}\left(\mathbf{B}_k\right) \in \mathbb{R}^{N_t l_k \times 1}$ and employing the following properties $\mathrm{Tr}(\mathbf{X}^H\mathbf{X}) = \mathrm{vec}(\mathbf{X})^H\mathrm{vec}(\mathbf{X}) = ||\mathrm{vec}(\mathbf{X})||_2^2$ and $\mathrm{vec}(\mathbf{XYZ}) = \left(\mathbf{Z}^T \otimes \mathbf{X}\right)\mathrm{vec}(\mathbf{Y})$ [52], the first term in (17) can be recast as

$$\mathrm{Tr}\left[\mathbf{A}^H \sum_{k=1}^{K} \widehat{\mathbf{H}}_k \mathbf{B}_k \mathbf{D}_k \boldsymbol{\Sigma}_\theta^{\frac{1}{2}} \boldsymbol{\Sigma}_\theta^{\frac{H}{2}} \left(\sum_{k=1}^{K} \widehat{\mathbf{H}}_k \mathbf{B}_k \mathbf{D}_k\right)^H \mathbf{A}\right] = \left|\left|\sum_{k=1}^{K} \left(\boldsymbol{\Sigma}_\theta^{\frac{1}{2}} \mathbf{G}^T \otimes \mathbf{A}^H \widehat{\mathbf{H}}_k\right) \mathbf{b}_k\right|\right|_2^2. \tag{30}$$

Upon exploiting the property $\mathrm{Tr}(\mathbf{P}^H\mathbf{QPR}) = \mathrm{vec}(\mathbf{P})^H\left(\mathbf{R}^T \otimes \mathbf{Q}\right)\mathrm{vec}(\mathbf{P})$, the various terms of (17) can be further simplified and the average MSE expression can be recast as

$$\overline{\mathrm{MSE}}\left(\{\mathbf{b}_k\}_{k=1}^K\right) = \left|\left|\sum_{k=1}^{K} \left(\boldsymbol{\Sigma}_\theta^{\frac{1}{2}} \mathbf{D}_k^T \otimes \mathbf{A}^H \widehat{\mathbf{H}}_k\right) \mathbf{b}_k\right|\right|_2^2 + \sum_{k=1}^{K} \mathbf{b}_k^H \boldsymbol{\Omega}_k \mathbf{b}_k - 2\Re\left(\sum_{k=1}^{K} \mathbf{c}_k^H \mathbf{b}_k\right), \tag{31}$$

where we have $\boldsymbol{\Omega}_k = \left(\alpha \mathbf{E}_k + \mathbf{U}_k + \mathbf{S}_k + \sigma_H^2 \mathbf{T}_k\right) \in \mathbb{R}^{l_k N_t \times l_k N_t}$. Furthermore, the scalar quantity $\alpha = \sigma_H^2 \mathrm{Tr}\left(\mathbf{A}^H\mathbf{A}\right)$ and the different matrices $\mathbf{E}_k \in \mathbb{R}^{l_k N_t \times l_k N_t}$, $\mathbf{U}_k \in \mathbb{R}^{l_k N_t \times l_k N_t}$, $\mathbf{S}_k \in \mathbb{R}^{l_k N_t \times l_k N_t}$, $\mathbf{T}_k \in \mathbb{R}^{l_k N_t \times l_k N_t}$ are defined as

$$\mathbf{E}_k = \left[\left[\mathbf{D}_k \boldsymbol{\Sigma}_\theta \mathbf{D}_k^H\right]^T \otimes \mathbf{I}_{N_t}\right] \tag{32}$$

$$\mathbf{U}_k = \left[\mathbf{I}_{l_k} \otimes \widehat{\mathbf{H}}_k^H \mathbf{A}\mathbf{A}^H \widehat{\mathbf{H}}_k\right] \tag{33}$$

$$\mathbf{S}_k = \left[\left[\widehat{\mathbf{H}}_k^H \mathbf{A}\mathbf{A}^H \mathbf{H}_k\right]^T \otimes \boldsymbol{\Psi}_k^e\right] \tag{34}$$

$$\mathbf{T}_k = \left[\left[\boldsymbol{\Psi}_k^e\right]^T \otimes \mathbf{I}_{N_t}\right], \tag{35}$$

where we have $\mathbf{c}_k = \mathrm{vec}\left(\widehat{\mathbf{H}}_k^H \mathbf{A} \boldsymbol{\Sigma}_\theta \mathbf{D}_k^H\right) \in \mathbb{R}^{l_k N_t \times 1}$. In a similar manner, one can also suitably modify the power constraint in (14). Hence, the final problem of determining the optimal MSE TPC matrices and energy covariance matrices can be readily formulated as

$$\begin{aligned} \underset{\{\mathbf{b}_k\}_{k=1}^K, \{\boldsymbol{\Phi}_j\}_{j=1}^J}{\text{minimize}} \quad & \overline{\mathrm{MSE}}\left(\{\mathbf{b}_k\}_{k=1}^K\right) \\ \text{subject to} \quad & t\gamma_{c,k} + t_I \mathbf{b}_k^H \boldsymbol{\Gamma}_k \mathbf{b}_k \le t_E \gamma_{h,k},\ \forall k \\ & \mathrm{Tr}(\boldsymbol{\Phi}_j) \le \gamma_{T,j}, \text{and } \boldsymbol{\Phi}_j \succeq \mathbf{0},\ \forall j, \end{aligned} \tag{36}$$

where we have $\boldsymbol{\Gamma}_k = \left(\left(\mathbf{D}_k \boldsymbol{\Sigma}_\theta \mathbf{D}_k^H + \boldsymbol{\Psi}_k^e\right)^T \otimes \mathbf{I}_{N_t}\right) \in \mathbb{R}^{l_k N_t \times l_k N_t}$. Due to the convex nature of the optimization problem in (36) it can be solved efficiently using a suitable interior point method [53]. After solving the above optimization problem, one obtains the optimal TPC vectors $\mathbf{b}_k$ for $k = 1, 2 \ldots, K$ and energy covariance matrices $\boldsymbol{\Phi}_j$ for $j = 1, 2 \ldots, J$. Furthermore, the optimal precoding matrices $\mathbf{B}_k$ corresponding to each SeN k can be derived by exploiting the relation $\mathrm{vec}_{N_t}^{-1}\left(\mathbf{b}_k\right)$. Algorithm 1 summarizes the proposed iterative approach conceived for optimal bit allocation and robust joint transceiver and energy covariance matrix design.

Algorithm 1 Robust joint transceiver, energy covariance matrices and quantization under Gaussian CSI uncertainty.

1: **Input**: Observation vector $\mathbf{y}(n)$, RC matrix $\mathbf{A}(n-1)$, precoding matrices $\{\mathbf{B}_k(n-1)\}_{k=1}^K$, maximum iterations $n_{\max} = 20$ and desired accuracy $\epsilon = 0.0001$, total bit budget $\mathcal{B}$.
2: **Initialization**: $n = 1$, initialize $\mathbf{A}(0)$ randomly, $\mathbf{B}_k(0) = \sqrt{\sum_{j=1}^{J} \frac{\gamma_{T,k}||\mathbf{F}_{k,j}||_F^2}{N_t N_j}} \mathbf{1}_{N_t N_j}$ for $k = 1, 2, \ldots, K$.
3: **while** $\| \widehat{\boldsymbol{\theta}}^{(n)} - \boldsymbol{\theta}^{(n)} \|_2 \geq \epsilon$ and $n < n_{max}$ **do**
4: Find the optimal number of bits $\beta_{l,k}^{\text{opt}}$ using (28) for each l and k.
5: Evaluate the RC matrix $\mathbf{A}(n)$ using (29).
6: Evaluate the optimal precoding vectors $\{\mathbf{b}_k(n)\}_{k=1}^K$ and energy covariance matrices $\{\boldsymbol{\Phi}_j(n)\}_{j=1}^J$ using (36).
7: Compute the matrices $\mathbf{B}_k = \mathrm{vec}_{N_t}^{-1}\left(\mathbf{b}_k\right)$, $\forall\ k$.
8: update $n = n + 1$.
9: **end while**
10: **Output**: $\beta_{l,k}^{\text{opt}}$, $\mathbf{A}$, $\{\mathbf{B}_k\}_{k=1}^K$ and $\{\boldsymbol{\Phi}_j\}_{j=1}^J$.

Remark: One can also follow an alternative approach where initially the SeN observations are quantized using uniform bit allocation and subsequently, a BCD based iterative algorithm is employed, which yields the optimal MSE TPC and RC matrices upon convergence. Finally, the optimal bit allocation is derived by minimizing the corresponding portion of the MSE expression, which depends on the quantization noise covariance matrix for the TPC and RC matrices obtained from the BCD algorithm. The proof of the theoretical convergence for this approach is given in subsection-IV-C.
The next Section develops a scheme for optimal bit allocation followed by our robust transceiver and energy covariance matrix design for the scenario, where the CSI uncertainty is bounded.

IV. Quantization and Robust Transceiver Design under Bounded CSI Uncertainty

In this scenario of bounded CSI uncertainty, the channel between the kth SeN and the FC can be modeled similar to (15), where the channel estimation error vector defined as $\Delta\mathbf{h}_k = \mathrm{vec}\left[\Delta\mathbf{H}_k\right] \in \mathbb{R}^{N_r N_T \times 1}$ satisfies

$$\Delta\mathbf{h}_k^H \mathbf{Q}_k \Delta\mathbf{h}_k \le \epsilon_H^2, \tag{37}$$

with ϵ_H representing the channel uncertainty radius and $\mathbf{Q}_k \in \mathbb{C}^{N_r N_T \times N_r N_T}$ is a positive definite matrix. Using the definition of Frobenius norm, i.e., $\mathrm{Tr}\left[\mathbf{X}\mathbf{X}^H\right] = ||\mathbf{X}||_F^2$, the

MSE expression in (13) can be equivalently written as

$$\text{MSE} = \left|\left|\left(\sum_{k=1}^{K}\mathbf{A}^H\mathbf{H}_k\mathbf{B}_k\mathbf{D}_k - \mathbf{I}\right)\boldsymbol{\Sigma}_\theta^{\frac{1}{2}}\right|\right|_F^2 + \sum_{k=1}^{K}\left|\left|\mathbf{A}^H\mathbf{H}_k\mathbf{B}_k\left(\boldsymbol{\Psi}_k^e\right)^{\frac{1}{2}}\right|\right|_F^2 + \left|\left|\mathbf{A}^H\boldsymbol{\Psi}_{\text{FC}}^{\frac{1}{2}}\right|\right|_F^2. \quad (38)$$

The next subsection derives the optimal bit allocation for the quantization of each SeN's observations assuming that the transceivers are known.

A. Optimal quantization of SeN observations for bounded CSI uncertainty scenario

Assuming that the RC and TPC matrices are known, this subsection develops a strategy for the optimal allocation of the given bit-rate budget to each SeN in the network, which ultimately results in the optimal quantization of the SeN measurements. To this end, upon substituting $\boldsymbol{\Psi}_k^e = \boldsymbol{\Psi}_k + \boldsymbol{\Psi}_k^q$, into (38), one obtains

$$\text{MSE} = \left|\left|\left(\sum_{k=1}^{K}\mathbf{A}^H\mathbf{H}_k\mathbf{B}_k\mathbf{D}_k - \mathbf{I}\right)\boldsymbol{\Sigma}_\theta^{\frac{1}{2}}\right|\right|_F^2 + \left|\left|\mathbf{A}^H\boldsymbol{\Psi}_{\text{FC}}^{\frac{1}{2}}\right|\right|_F^2 + \sum_{k=1}^{K}\left|\left|\mathbf{A}^H\mathbf{H}_k\mathbf{B}_k\boldsymbol{\Psi}_k^{\frac{1}{2}}\right|\right|_F^2 + \sum_{k=1}^{K}\left|\left|\mathbf{A}^H\mathbf{H}_k\mathbf{B}_k\left(\boldsymbol{\Psi}_k^q\right)^{\frac{1}{2}}\right|\right|_F^2. \quad (39)$$

It can now be readily observed from the MSE expression above that only the term $\sum_{k=1}^{K}\left|\left|\mathbf{A}^H\mathbf{H}_k\mathbf{B}_k\left(\boldsymbol{\Psi}_k^q\right)^{\frac{1}{2}}\right|\right|_F^2$ depends on the quantization noise covariance matrix, which can be further optimized to minimize the resultant MSE at the FC. This term can be written equivalently as

$$\sum_{k=1}^{K}\left|\left|\mathbf{A}^H\mathbf{H}_k\mathbf{B}_k\left(\boldsymbol{\Psi}_k^q\right)^{\frac{1}{2}}\right|\right|_F^2 = ||\mathbf{e}^q||_2^2, \quad (40)$$

where the vector $\mathbf{e}^q \in \mathbb{R}^{\tilde{m}\times 1}$ is defined as

$$\mathbf{e}^q = \begin{bmatrix}\text{vec}\left(\mathbf{A}^H\mathbf{H}_1\mathbf{B}_1\left(\boldsymbol{\Psi}_1^q\right)^{\frac{1}{2}}\right)\\ \vdots \\ \text{vec}\left(\mathbf{A}^H\mathbf{H}_K\mathbf{B}_K\left(\boldsymbol{\Psi}_K^q\right)^{\frac{1}{2}}\right)\end{bmatrix}, \quad (41)$$

with $\tilde{m} = m(m + Kl + N_r)$. Once again, on account of CSI uncertainty, substituting $\mathbf{H}_k = \widehat{\mathbf{H}}_k + \Delta\mathbf{H}_k$ in (41), the vector $\mathbf{e}^q$ can be recast as

$$\mathbf{e}^q = \widehat{\mathbf{e}}^q + \sum_{k=1}^{K}\mathbf{E}_{H_k}^q\mathbf{Q}_k^{-T/2}\mathbf{Q}_k^{1/2}\Delta\mathbf{h}_k, \quad (42)$$

where the matrix $\mathbf{E}_{H_k}^q \in \mathbb{R}^{m(m+Kl)\times N_rN_t}$ and the vector $\widehat{\mathbf{e}}^q \in \mathbb{R}^{\tilde{m}\times 1}$ are defined as

$$\mathbf{E}_{H_k}^q = \begin{bmatrix}\mathbf{0}_{Kl(k-1)m\times N_tN_r}\\ \left(\mathbf{B}_k\left(\boldsymbol{\Psi}_k^q\right)^{\frac{1}{2}}\right)^T\otimes\mathbf{A}^H\\ \vdots \\ \mathbf{0}_{(Klk+1)m\times N_tN_r.}\end{bmatrix}, \quad (43)$$

$$\widehat{\mathbf{e}}^q = \begin{bmatrix}\text{vec}\left(\mathbf{A}^H\widehat{\mathbf{H}}_1\mathbf{B}_1\left(\boldsymbol{\Psi}_1^q\right)^{\frac{1}{2}}\right)\\ \vdots \\ \text{vec}\left(\mathbf{A}^H\widehat{\mathbf{H}}_K\mathbf{B}_K\left(\boldsymbol{\Psi}_K^q\right)^{\frac{1}{2}}\right)\end{bmatrix}. \quad (44)$$

Hence, the optimization problem to minimize the quantity $\mathbf{e}^q$ subject to a total bit-rate budget constraint $\mathcal{B}$ can be readily formulated as

$$\begin{aligned}\underset{\boldsymbol{\beta}}{\text{minimize}} \quad & ||\mathbf{e}^q||_2^2 \\ \text{subject to} \quad & \mathbf{1}^T\boldsymbol{\beta} \le \mathcal{B}.\end{aligned} \quad (45)$$

The above optimization can be further modified using the epigraph form as [51]

$$\begin{aligned}\underset{\boldsymbol{\beta}}{\text{minimize}} \quad & \tau^q \\ \text{subject to} \quad & ||\mathbf{e}^q||_2^2 \le \tau^q \\ & \mathbf{1}^T\boldsymbol{\beta} \le \mathcal{B}.\end{aligned} \quad (46)$$

The first constraint in the above optimization problem in (46) can further be written as $\tau^q - ||\mathbf{e}^q||_2^2 \ge 0$, which can also be modified as

$$\begin{bmatrix}\tau^q & (\mathbf{e}^q)^H\\ \mathbf{e}^q & \mathbf{I}_{\tilde{m}}\end{bmatrix} \succeq 0. \quad (47)$$

Substituting the value of $\mathbf{e}^q$ from (42), one obtains

$$\begin{bmatrix}\tau^q & (\widehat{\mathbf{e}}^q)^H\\ \widehat{\mathbf{e}}^q & \mathbf{I}_{\tilde{m}}\end{bmatrix} \ge -\sum_{k=1}^{K}\begin{bmatrix}0 & \left(\mathbf{E}_{H_k}^q\text{vec}\left(\Delta\mathbf{H}_k\right)\right)^H\\ \left(\mathbf{E}_{H_k}^q\text{vec}\left(\Delta\mathbf{H}_k\right)\right) & \mathbf{0}_{m(m+Kl)\times m(m+Kl)}\end{bmatrix}. \quad (48)$$

Furthermore, upon employing the following Lemma-2, one can recast the above constraint in the form of a linear matrix inequality (LMI).

Lemma 2: Given the matrices $\mathbf{P}$ and $\{\mathbf{M}_k, \mathbf{N}_k\}_{k=1}^K$ with $\mathbf{P} = \mathbf{P}^H$, the semi-infinite LMI of the form [54]

$$\mathbf{P} \succeq \sum_{k=1}^{K}\left(\mathbf{M}_k^H\mathbf{X}_k\mathbf{N}_k + \mathbf{N}_k^H\mathbf{X}_k^H\mathbf{M}_k\right),\ \forall k, \mathbf{X}_k : \|\mathbf{X}_k\| \le \epsilon_k \quad (49)$$

holds if and only if there exist non-negative real numbers $\mu_1, \ldots, \mu_K$ such that

$$\begin{bmatrix}\mathbf{P} - \sum_{k=1}^{K}\mu_k\mathbf{N}_k^H\mathbf{N}_k & -\epsilon_1\mathbf{M}_1^H & \cdots & -\epsilon_K\mathbf{M}_K^H\\ -\epsilon_1\mathbf{M}_1 & \mu_1\mathbf{I} & \cdots & \mathbf{0}\\ \vdots & \vdots & \ddots & \vdots\\ -\epsilon_K\mathbf{M}_K & \mathbf{0} & \cdots & \mu_K\mathbf{I}\end{bmatrix} \succeq 0. \quad (50)$$

The matrix norm in this lemma is the spectral norm. But, in our problem formulation, since $\mathbf{X}_k$ is a vector quantity, the spectral norm is equal to the Frobenius norm. Hence, employing Lemma-2, one can write (48) in the form of an LMI, as shown next. Upon comparing (48) and (49), Eq. (48) can be recast as

$$\begin{bmatrix} \mathbf{\Sigma} & -\epsilon_H \left(\mathbf{M}_1^q\right)^H & \cdots & -\epsilon_H \left(\mathbf{M}_K^q\right)^H \\ -\epsilon_H \mathbf{M}_1^q & \mu_1 \mathbf{I} & \cdots & \mathbf{0} \\ \vdots & \vdots & \ddots & \vdots \\ -\epsilon_H \mathbf{M}_K^q & \mathbf{0} & \cdots & \mu_K \mathbf{I} \end{bmatrix} \succeq 0, \quad (51)$$

where the matrices $\mathbf{\Sigma} \in \mathbb{R}^{\tilde{m}+1 \times \tilde{m}+1}$, $\mathbf{W}^q \in \mathbb{R}^{\tilde{m}+1 \times \tilde{m}+1}$, $\mathbf{M}_k^q \in \mathbb{R}^{N_r N_t \times (K+2)N_t^2}$ and $\mathbf{N}_k^q \in \mathbb{R}^{1 \times \tilde{m}+1}$ are defined as

$$\mathbf{\Sigma} = \begin{bmatrix} \tau^q - \sum_{k=1}^{K} \mu_k & \left(\widehat{\mathbf{e}}^q\right)^H \\ \widehat{\mathbf{e}}^q & \mathbf{I}_{\tilde{m}} \end{bmatrix} \quad (52)$$

$$\mathbf{P}^q = \begin{bmatrix} \tau^q & \left(\widehat{\mathbf{e}}^q\right)^H \\ \widehat{\mathbf{e}}^q & \mathbf{I}_{\tilde{m}} \end{bmatrix} \quad (53)$$

$$\mathbf{M}_k^q = \begin{bmatrix} \mathbf{0}_{N_{FC} N_S \times 1} & \mathbf{Q}_k^{-T/2} \left(\mathbf{E}_{H_k}^q\right)^H \end{bmatrix} \quad (54)$$

$$\mathbf{N}_k^q = \begin{bmatrix} -1 & \mathbf{0}_{N_r N_t \times \tilde{m}} \end{bmatrix}^T. \quad (55)$$

Hence, the final optimization problem to determine the bit allocation vector $\boldsymbol{\beta}$ toward quantization of the SeN observations, subject to a total bit-rate constraint, can be formulated as

$$\begin{aligned} \underset{\boldsymbol{\beta}}{\text{minimize}} \quad & \tau^q \\ \text{subject to} \quad & (51), \text{ and } \mathbf{1}^T \boldsymbol{\beta} \leq \mathcal{B}. \end{aligned} \quad (56)$$

Once, the optimal bit allocation vector is derived, the next subsection discusses the robust transceiver and energy covariance matrices design for this bounded CSI uncertainty scenario.

B. Robust Transceiver and Energy Covariance Matrices design

This subsection develops an iterative framework for designing the robust transceiver and energy covariance matrices for MSE minimization at the FC relying on quantized SeN observation transmission. To this end, exploiting the property that $||\mathbf{X}||_F^2 = ||\mathbf{x}||_2^2$, one can recast the MSE expression in (38) as

$$\text{MSE} = ||\mathbf{e}||_2^2, \quad (57)$$

where the vector $\mathbf{e} \in \mathbb{R}^{\tilde{m} \times 1}$ is defined as

$$\mathbf{e} = \begin{bmatrix} \text{vec}\left(\sum_{k=1}^{K} \mathbf{A}^H \mathbf{H}_k \mathbf{B}_k \mathbf{D}_k \mathbf{\Sigma}_\theta^{\frac{1}{2}}\right) - \text{vec}\left(\mathbf{\Sigma}_\theta\right) \\ \text{vec}\left(\mathbf{A}^H \mathbf{H}_1 \mathbf{B}_1 \left(\mathbf{\Psi}_1^e\right)^{\frac{1}{2}}\right) \\ \vdots \\ \text{vec}\left(\mathbf{A}^H \mathbf{H}_K \mathbf{B}_K \left(\mathbf{\Psi}_K^e\right)^{\frac{1}{2}}\right) \\ \text{vec}\left(\mathbf{A}^H \mathbf{\Psi}_{\text{FC}}^{\frac{1}{2}}\right) \end{bmatrix}. \quad (58)$$

Now, substituting $\mathbf{H}_k = \widehat{\mathbf{H}}_k + \Delta\mathbf{H}_k$ in the above expression, and exploiting the property $\text{vec}\left(\mathbf{XYZ}\right) = \left(\mathbf{Z}^T \otimes \mathbf{X}\right) \text{vec}\left(\mathbf{Y}\right)$, one can rewrite the expression for the vector $\mathbf{e}$ as

$$\mathbf{e} = \widehat{\mathbf{e}} + \sum_{k=1}^{K} \mathbf{E}_{H_k} \mathbf{Q}_k^{-H/2} \mathbf{Q}_k^{1/2} \Delta\mathbf{h}_k, \quad (59)$$

where the quantities $\widehat{\mathbf{e}} \in \mathbb{R}^{\tilde{m} \times 1}$ and $\mathbf{E}_{H_K} \in \mathbb{R}^{m(m+Kl) \times N_r N_t}$ are defined as

$$\widehat{\mathbf{e}} = \begin{bmatrix} \text{vec}\left(\sum_{k=1}^{K} \mathbf{A}^H \widehat{\mathbf{H}}_k \mathbf{B}_k \mathbf{D}_k \mathbf{\Sigma}_\theta^{\frac{1}{2}}\right) - \text{vec}\left(\mathbf{\Sigma}_\theta\right) \\ \text{vec}\left(\mathbf{A}^H \widehat{\mathbf{H}}_1 \mathbf{B}_1 \left(\mathbf{\Psi}_1^e\right)^{\frac{1}{2}}\right) \\ \vdots \\ \text{vec}\left(\mathbf{A}^H \widehat{\mathbf{H}}_K \mathbf{B}_K \left(\mathbf{\Psi}_K^e\right)^{\frac{1}{2}}\right) \\ \text{vec}\left(\mathbf{A}^H \mathbf{\Psi}_{\text{FC}}^{\frac{1}{2}}\right) \end{bmatrix}, \quad (60)$$

$$\mathbf{E}_{H_k} = \begin{bmatrix} \left(\left(\mathbf{B}_k \mathbf{D}_k \mathbf{\Sigma}_\theta^{\frac{1}{2}}\right)^T \otimes \mathbf{A}^H\right) \\ \mathbf{0}_{Kl(k-1)m \times N_t N_r} \\ \left(\mathbf{B}_k \left(\mathbf{\Psi}_k^e\right)^{\frac{1}{2}}\right)^T \otimes \mathbf{A}^H \\ \vdots \\ \mathbf{0}_{(Klk+1)m \times N_t N_r} \end{bmatrix}. \quad (61)$$

Hence, the optimization problem of minimizing the MSE in (57) subject to per SeN power constraints is given by

$$\begin{aligned} \underset{\mathbf{A}, \{\mathbf{B}_k\}_{k=1}^K, \{\mathbf{\Phi}_j\}_{j=1}^J}{\text{minimize}} \quad & ||\mathbf{e}||_2^2 & (61a) \\ \text{subject to} \quad & t\gamma_{C,k} + t_I \text{Tr}(\mathbf{B}_k \left[\mathbf{D}_k \mathbf{\Sigma}_\theta \mathbf{D}_k^H + \mathbf{\Psi}_k^e\right] \mathbf{B}_k^H] \\ & \leq t_E \gamma_{H,k}, \forall k, & (61b) \\ & \text{Tr}\left[\mathbf{\Phi}_j\right] \leq P_{T,j}, \text{and } \mathbf{\Phi}_j \succeq \mathbf{0}, \forall j. & (61c) \end{aligned}$$

The above optimization problem is intractable as it stands. Hence, employing the epigraph form of [51], the above optimization problem can be modified as

$$\begin{aligned} \underset{\mathbf{A}, \{\mathbf{B}_k\}_{k=1}^K, \{\mathbf{\Phi}_j\}_{j=1}^J, \tau}{\text{minimize}} \quad & \tau \\ \text{subject to} \quad & ||\mathbf{e}||_2^2 \leq \tau \\ & (61b), \text{ and } (61c). \end{aligned} \quad (62)$$

The first constraint in (62) can further be recast as the linear matrix inequality (LMI) below

$$\tau - ||\mathbf{e}||_2^2 = \begin{bmatrix} \tau & \mathbf{e}^H \\ \mathbf{e} & \mathbf{I}_{\tilde{m}} \end{bmatrix} \succeq 0. \quad (63)$$

Substituting the value of $\mathbf{e}$ from (59) into the above LMI, one obtains

$$\begin{bmatrix} \tau & \widehat{\mathbf{e}}^H \\ \widehat{\mathbf{e}} & \mathbf{I}_{\tilde{m}} \end{bmatrix} \geq -\sum_{k=1}^{K} \begin{bmatrix} 0 & \left(\mathbf{E}_{H_k} \text{vec}\left(\Delta\mathbf{H}_k\right)\right)^H \\ \left(\mathbf{E}_{H_k} \text{vec}\left(\Delta\mathbf{H}_k\right)\right) & \mathbf{0}_{m(m+Kl) \times m(m+Kl)} \end{bmatrix}. \quad (64)$$

It can be seen that (64) is similar to (49), and hence, the expression in (64) can be recast as

$$\begin{bmatrix} \begin{bmatrix} \tau - \sum_{k=1}^{K} \mu_k & \widehat{\mathbf{e}}^H \\ \widehat{\mathbf{e}} & \mathbf{I} \end{bmatrix} & \begin{matrix} -\epsilon_H \mathbf{M}_1^H & \cdots & -\epsilon_H \mathbf{M}_K^H \end{matrix} \\ \begin{matrix} -\epsilon_H \mathbf{M}_1 \\ \vdots \\ -\epsilon_H \mathbf{M}_K \end{matrix} & \begin{matrix} \mu_1 \mathbf{I} & \cdots & \mathbf{0} \\ \vdots & \ddots & \vdots \\ \mathbf{0} & \cdots & \mu_K \mathbf{I} \end{matrix} \end{bmatrix} \succeq 0, \tag{65}$$

where the matrices $\mathbf{P} \in \mathbb{R}^{\tilde{m}+1 \times \tilde{m}+1}$, $\mathbf{M}_k \in \mathbb{R}^{N_r N_t \times (K+2)N_t^2}$ and $\mathbf{N}_k \in \mathbb{R}^{1 \times \tilde{m}+1}$ are defined as

$$\begin{aligned} \mathbf{P} &= \begin{bmatrix} \tau & \widehat{\mathbf{e}}^H \\ \widehat{\mathbf{e}} & \mathbf{I}_{\tilde{m}} \end{bmatrix}, \\ \mathbf{M}_k &= \begin{bmatrix} \mathbf{0}_{N_r N_t \times 1} & \mathbf{Q}_k^{-T/2} \mathbf{E}_{H_k}^H \end{bmatrix}, \ \mathbf{N}_k = [-1 \quad \mathbf{0}_{1 \times \tilde{m}}]^T. \end{aligned} \tag{66}$$

Hence, the final optimization problem is

$$\begin{aligned} \underset{\mathbf{A}, \{\mathbf{B}_k\}_{k=1}^K, \{\mathbf{\Phi}_j\}_{j=1}^J}{\text{minimize}} \quad & \tau \\ \text{subject to} \quad & (65),\ (61b),\ \text{and}\ (61c). \end{aligned} \tag{67}$$

The above optimization problem is once again non-convex in nature due to coupling of the optimization variables. Hence, BCD-based iterative framework can be invoked where the optimization problem to determine robust combining matrix $\mathbf{A}$ for the given TPC matrices $\{\mathbf{B}_k\}_{k=1}^K$ and energy covariance matrices $\{\mathbf{\Phi}_j\}_{j=1}^J$ is

$$\begin{aligned} \underset{\mathbf{A}, \{\mathbf{B}_k\}_{k=1}^K, \{\mathbf{\Phi}_j\}_{j=1}^J}{\text{minimize}} \quad & \tau \\ \text{subject to} \quad & (65). \end{aligned} \tag{68}$$

Moreover, the optimization problem to drtermine optimal TPC and energy covaraince matrices for a given RC matrix $\mathbf{A}$ can be formulated as

$$\begin{aligned} \underset{\{\mathbf{B}_k\}_{k=1}^K, \{\mathbf{\Phi}_j\}_{j=1}^J}{\text{minimize}} \quad & \tau \\ \text{subject to} \quad & (65),\ (61b),\ \text{and}\ (61c). \end{aligned} \tag{69}$$

Algorithm 2 summarizes the proposed approach. The next subsection provides a theoretical proof of the algorithm's convergence.

C. Convergence analysis

This subsection proves the theoretical convergence of the proposed scheme where initially uniform bit allocation based quantization is performed, followed by BCD-based optimal transceiver design. On convergence, optimal bit allocation is performed, which further minimizes the MSE for the given transceivers. Since, the problem designing the optimal RC and TPC matrices in (18) and (36) for the Gaussian, and (67) for the bounded CSI uncertainty models, are convex in nature, the following inequalities hold:

$$\begin{aligned} &\overline{\text{MSE}}\Big(\{\mathbf{A}\}^{(n)}, \{\mathbf{B}_k\}^{(n)}, \{\mathbf{\Phi}_j\}^{(n)}\Big) \\ &\geq \min_{\mathbf{A}} \overline{\text{MSE}}\Big(\mathbf{A} | \{\mathbf{B}_k\}^{(n)}, \{\mathbf{\Phi}_j\}^{(n)}\Big) \\ &= \overline{\text{MSE}}\Big(\mathbf{A}^{(n+1)}, \{\mathbf{B}_k\}^{(n)}, \{\mathbf{\Phi}_j\}^{(n)}\Big) \\ &\geq \min_{\mathbf{B}_k, \mathbf{\Phi}_j} \overline{\text{MSE}}\Big(\mathbf{B}_k, \mathbf{\Phi}_j | \{\mathbf{A}\}^{(n+1)}\Big) \\ &= \overline{\text{MSE}}\Big(\{\mathbf{B}_k\}^{(n+1)}, \{\mathbf{\Phi}_j\}^{(n+1)}, \{\mathbf{A}\}^{(n+1)}\Big). \end{aligned} \tag{70}$$

The sequence $\overline{\text{MSE}}\Big(\{\mathbf{A}\}^{(n)}, \{\mathbf{B}_k\}^{(n)}, \{\mathbf{\Phi}_j\}^{(n)}\Big)$ is monotonically decreasing and it is lower bounded by zero. This proves that the algorithm converges.

Algorithm 2 Robust joint transceiver, energy covaraince matrices and quantization under bounded CSI uncertainty.

1: **Input**: Observation vector $\mathbf{y}(n)$, RC matrix $\mathbf{A}(n-1)$, precoding matrices $\{\mathbf{B}_k(n-1)\}_{k=1}^K$, maximum iterations $n_{\max} = 20$ and desired accuracy $\epsilon = 0.0001$, total bit budget $\mathcal{B}$.
2: **Initialization**: $n = 1$, initialize $\mathbf{A}(0)$ randomly, $\mathbf{B}_k(0) = \sqrt{\sum_{j=1}^J \frac{\gamma_{T,k} ||\mathbf{F}_{k,j}||_F^2}{N_t N_j}} \mathbf{1}_{N_t N_j}$ for $k = 1, 2, \ldots, K$.
3: **while** $\| \widehat{\boldsymbol{\theta}}^{(n)} - \boldsymbol{\theta}^{(n)} \|_2 \geq \epsilon$ and $n < n_{max}$ **do**
4: Find the optimal bit allocation vector $\boldsymbol{\beta}$ from (56).
5: Evaluate the RC matrix $\mathbf{A}(n)$ using (68).
6: Evaluate the optimal precoding matrices $\{\mathbf{B}_k(n)\}_{k=1}^K$ and energy covariance matrices $\{\mathbf{\Phi}_j(n)\}_{j=1}^J$ by solving (69).
7: update $n = n + 1$.
8: **end while**
9: **Output**: $\boldsymbol{\beta}$, $\mathbf{A}$, $\{\mathbf{B}_k\}_{k=1}^K$ and $\mathbf{\Sigma}_j$ for $j = 1, 2 \ldots, J$.

D. Computation Complexity Analysis

The overall computational complexity of the proposed scheme for the scenario with Gaussian CSI uncertainty modelling is $\mathcal{O}\left((KN_t l + JN_j^2)^{3.5}\right) + \mathcal{O}(N_r^3)$, where the first term arises from the worst case complexity of the optimization problem in (36) assuming $l_k = l$ for all the SeNs in the EH-IoTNe [28]. The second term can be attributed to the complexity incurred in the computation of the robust combining matrix using (29). Furthermore, for the scenario with bounded CSI uncertainty, the overall complexity is $\mathcal{O}\left((N_r^3 m^6)\right) + \mathcal{O}\left((N_t^2 K^2 l^2 + J^2 N_j^2) N_r^2 m^2\right)$, where the first term arises from the computational complexity of deriving optimal robust combining matrix $\mathbf{A}$. Whereas the second term represents the computational requirement of determining optimal precoding and energy covariance matrices $\{\mathbf{B}_k\}_{k=1}^K$, and $\{\mathbf{\Phi}_j\}_{j=1}^J$, respectively [56].

V. Simulation Results

The elements of the wireless fading channels $\mathbf{F}_j$ for each EAP j and $\mathbf{H}_k$ for each SeN k are generated as $\mathcal{N}(0, 1)$. The unknown parameter of interest $\boldsymbol{\theta}$ is generated according

Parameter	Value
Number of SeNs (K)	15
Number of EAPs (J)	4
Number of antennas at each SeN (N_t)	2
Number of antennas at each EAP (N_j)	4
Number of antennas at the FC (N_r)	2
Number of elements in the parameter vector $\boldsymbol{\theta}$ (m)	2
Energy harvesting efficiency for each SeN k (ζ_k)	0.75
Circuit power consumption for each SeN k ($\gamma_{c,k}$)	-47 dBm
Observation SNR (SNR_{OB})	10 dB
SNR at the FC (SNR_{FC})	20 dB

TABLE II
SUMMARY OF THE SIMULATION SETUP

to $\mathcal{N}(\mathbf{0}, \mathbf{I}_m)$, where $m = 2$. The number of antennas at each EAP and SeN are set to 4 and 2, respectively, while the FC is equipped with 2 antennas. The observation SNR denoted by SNR_{OB} is set as 10 dB, while the SNR at the FC, denoted as SNR_{FC}, is considered to be 20 dB. The total time t is set to 1 and divided equally between the energy harvesting and information transfer intervals, i.e., $t_I = t_E = 0.5$. The energy harvesting efficiency for each SeN k is set to $\zeta_k = 0.75$. The circuit power consumption at each SeN k is assumed to be $\gamma_{c,k} = -47$ dBm. The number of SeNs and EAPs considered are $K = 15$ and $J = 4$, respectively. Furthermore, from the performance comparison point of view, the perfect and imperfect CSI plots have been obtained by extending the algorithm in [20] for a quantized sensor observation scenario. A concise summary of the simulation setup is given in Table II.

The convergence performance of the two approaches proposed in Section-III for the case of Gaussian CSI uncertainty is shown in Fig. 2. In Approach 1, the robust transceivers are initially obtained for the uniform bit allocation based quantized SeN observations, and then the optimal bit allocation is derived for the given transceivers. On the other side, with Approach 2, optimal bit allocation is performed first and subsequently, the robust transceivers are designed. The result indicates that both the approaches produce almost similar MSE performance. It can be readily inferred that the robust design outperforms the uncertainty agnostic or imperfect CSI-based design.

Fig. 3 compares the MSEs of the proposed optimal bit-rate allocation based quantization in Section-III and uniform bit allocation based scheme wherein the total bit-rate budget is distributed equally among the SeNs. As it becomes evident from the figure, the optimal bit allocation based intelligent quantization scheme outperforms the uniform bit allocation based quantization scheme. It can also be observed form the figure that the proposed robust design performs quite similar to the perfect CSI scenario, which demonstrates the effectiveness of the conceived design.

Fig. 4 characterizes the MSE performance of the proposed robust joint transceiver and energy covariance matrices relying on the optimal bit allocation based quantization procedure developed in Section-III versus the different transmit power levels gleaned from each EAP in the network. It can be observed that the proposed robust design outperforms the imperfect CSI-based design in terms of its MSE and indeed, it approaches the perfect CSI-based design. This confirms the

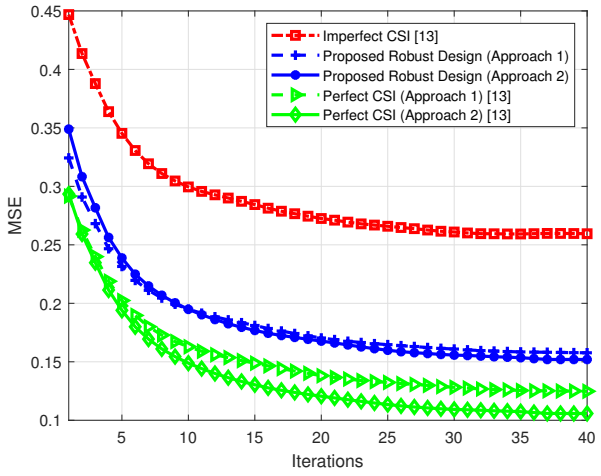

Fig. 2. MSE versus number of iterations for the Gaussian CSI uncertainty model.

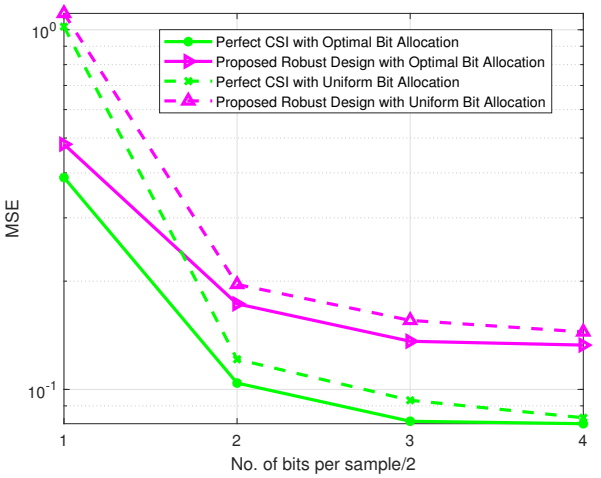

Fig. 3. MSE versus number of bits for the Gaussian CSI uncertainty model.

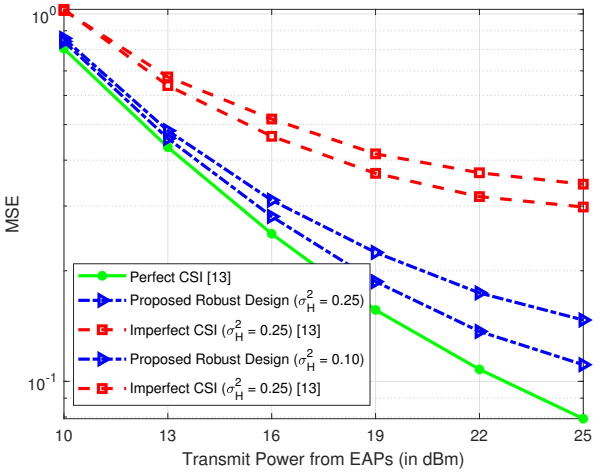

Fig. 4. MSE versus the power transmitted from each EAP for the Gaussian CSI uncertainty model.

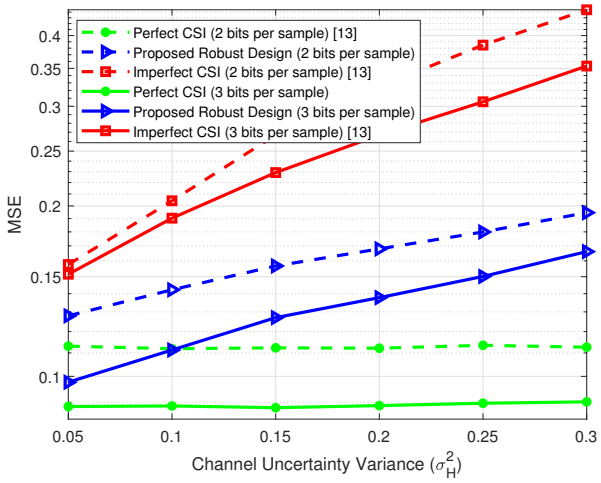

Fig. 5. MSE versus varying channel uncertainty variance ($\boldsymbol{\sigma_H^2}$) for the Gaussian CSI uncertainty model.

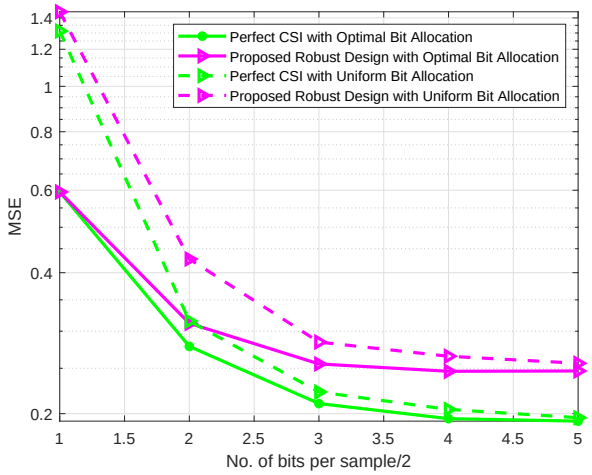

Fig. 7. MSE versus number of bits for the bounded CSI uncertainty model.

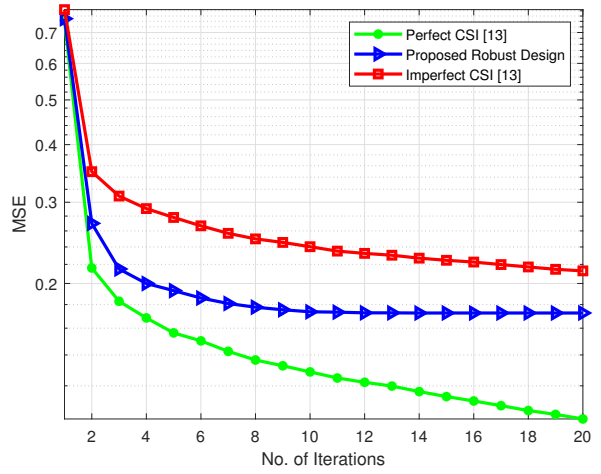

Fig. 6. MSE versus number of iterations for the bounded CSI uncertainty model.

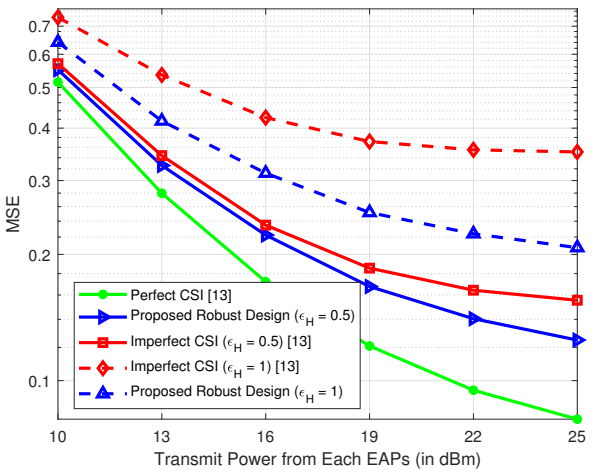

Fig. 8. MSE versus transmitted power from each EAP for the bounded CSI uncertainty model.

advantages of the robust design proposed.

Fig. 5 displays the MSE performance of the robust design conceived versus the channel uncertainty variance σ_H^2 for different bits-per-sample values. As expected, the MSE performance improves as the number of bits per sample increases. It can once again be seen that the proposed scheme performs close to the perfect CSI based scheme and outperforms the uncertainty agnostic design. It is also clear that as the power transmitted from the EAP increases, the SeNs can harvest more energy and therefore the estimation performance improves.

Fig. 6 depicts the convergence performance of the iterative approach developed in Section-IV for the bounded CSI uncertainty model. It can be readily observed that the proposed approach converges after 10 iterations and offers a better MSE performance than the uncertainty agnostic design. Fig. 7 plots the MSE performance of the optimal bit allocation based quantization scheme with the uniform bit allocation scheme. It can once again be deduced that the optimal bit allocation scheme outperforms the uniform bit allocation scheme. As expected, the performance gap is significant for a lower number of bits and decreases as the number of bits increases.

Fig. 8 demonstrates the MSE performance of the proposed algorithm for robust joint transceiver and energy covariance matrix design as a function of the different transmit power levels from each EAP in the EH-IoTNe. It can be seen that the proposed robust design offers significant MSE performance improvement over the imperfect CSI based design and performs similarly to the ideal perfect CSI based design. Furthermore, as the uncertainty radius grows, the performance gap between the suggested robust and uncertainty agnostic design increases dramatically, demonstrating again the proposed robust design's efficacy.

Fig. 9 shows the MSE performance of the suggested robust design versus the channel uncertainty radius ϵ_H for various values of the number of SeNs in the EH-IoTNe. Once again, it is clear that the suggested scheme outperforms the uncertainty agnostic design and does not deviate much from a perfect CSI-based scheme. It can also be shown that when the number

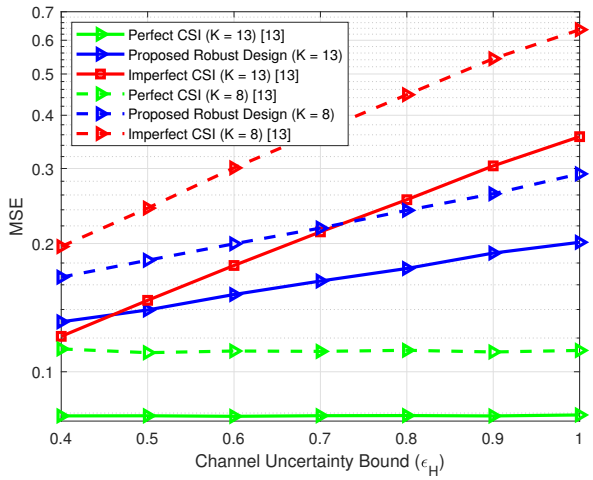

Fig. 9. MSE versus varying channel uncertainty bound (ϵ_H) for the bounded CSI uncertainty model.

of SeNs increases, the estimation performance inevitably gets better because there are more observations available at the FC.

VI. Conclusions

In this paper, considering an energy harvesting IoTNe, BCD-based iterative approaches were developed for optimal bit allocation and robust transceiver design based on MSE minimization at the FC. The proposed schemes also take into account the inadequacy of the available CSI, which has been characterized using both Gaussian and bounded uncertainty models. For the Gaussian CSI uncertainty model, closed-form expressions for optimal bit allocation and the RC matrix were derived, and a QCQP-based optimization problem was formulated and solved in order to determine the robust TPC matrices. In addition, for the scenario of bounded CSI uncertainty, two distinct optimization problems were formulated in order to derive the optimal bit allocation and robust transceivers, respectively. Explicit theoretical convergence results were proved for the proposed approaches. Our simulation results demonstrated the superiority of the proposed robust designs over their conventional uncertainty-agnostic counterpart, in which only the estimated channel is used to design the transceivers and the energy covariance matrices, with no consideration of the CSI uncertainty.

References

[1] J.-Y. Kim, C.-H. Chu, and M.-S. Kang, "IoT-based unobtrusive sensing for sleep quality monitoring and assessment," *IEEE Sensors Journal*, vol. 21, no. 3, pp. 3799–3809, 2021.

[2] Y. Zi, L. Fan, X. Wu, J. Chen, and Z. Han, "Distributionally robust optimal sensor placement method for site-scale methane-emission monitoring," *IEEE Sensors Journal*, vol. 22, no. 23, pp. 23 403–23 412, 2022.

[3] H.-C. Chang, Y.-L. Hsu, C.-Y. Hsiao, and Y.-F. Chen, "Design and implementation of an intelligent autonomous surveillance system for indoor environments," *IEEE Sensors Journal*, vol. 21, no. 15, pp. 17 335–17 349, 2021.

[4] S. Amendola, G. Bovesecchi, A. Palombi, P. Coppa, and G. Marrocco, "Design, calibration and experimentation of an epidermal RFID sensor for remote temperature monitoring," *IEEE Sensors Journal*, vol. 16, no. 19, pp. 7250–7257, 2016.

[5] O. Khutsoane, B. Isong, N. Gasela, and A. M. Abu-Mahfouz, "WaterGrid-Sense: A LoRa-based sensor node for industrial IoT applications," *IEEE Sensors Journal*, vol. 20, no. 5, pp. 2722–2729, 2020.

[6] R. Saha, A. Chakraborty, S. Misra, S. K. Das, and C. Chatterjee, "DLSense: Distributed learning-based smart virtual sensing for precision agriculture," *IEEE Sensors Journal*, vol. 21, no. 16, pp. 17 556–17 563, 2021.

[7] P.-Y. Kong, "Cellular-assisted device-to-device communications for healthcare monitoring wireless body area networks," *IEEE Sensors Journal*, vol. 20, no. 21, pp. 13 139–13 149, 2020.

[8] J. Hu, K. Yang, G. Wen, and L. Hanzo, "Integrated data and energy communication network: A comprehensive survey," *IEEE Communications Surveys Tutorials*, vol. 20, no. 4, pp. 3169–3219, 2018.

[9] J.-J. Xiao, S. Cui, Z.-Q. Luo, and A. J. Goldsmith, "Linear coherent decentralized estimation," *IEEE Transactions on Signal Processing*, vol. 56, no. 2, pp. 757–770, 2008.

[10] S. Kar and P. K. Varshney, "Linear coherent estimation with spatial collaboration," *IEEE Transactions on Information Theory*, vol. 59, no. 6, pp. 3532–3553, 2013.

[11] S. Liu, S. Kar, M. Fardad, and P. K. Varshney, "Sparsity-aware sensor collaboration for linear coherent estimation," *IEEE Transactions on Signal Processing*, vol. 63, no. 10, pp. 2582–2596, 2015.

[12] ——, "Optimized sensor collaboration for estimation of temporally correlated parameters," *IEEE Transactions on Signal Processing*, vol. 64, no. 24, pp. 6613–6626, 2016.

[13] X. Lu, P. Wang, D. Niyato, D. I. Kim, and Z. Han, "Wireless charging technologies: Fundamentals, standards, and network applications," *IEEE Communications Surveys Tutorials*, vol. 18, no. 2, pp. 1413–1452, 2016.

[14] M. Nourian, S. Dey, and A. Ahlén, "Distortion minimization in multi-sensor estimation with energy harvesting," *IEEE Journal on Selected Areas in Communications*, vol. 33, no. 3, pp. 524–539, 2015.

[15] Z. Wang, L. Duan, and R. Zhang, "Adaptively directional wireless power transfer for large-scale sensor networks," *IEEE Journal on Selected Areas in Communications*, vol. 34, no. 5, pp. 1785–1800, 2016.

[16] H. Zhou, T. Jiang, C. Gong, and Y. Zhou, "Optimal estimation in wireless sensor networks with energy harvesting," *IEEE Transactions on Vehicular Technology*, vol. 65, no. 11, pp. 9386–9396, 2016.

[17] S. Guo, F. Wang, Y. Yang, and B. Xiao, "Energy-efficient cooperative tfor simultaneous wireless information and power transfer in clustered wireless sensor networks," *IEEE Transactions on Communications*, vol. 63, no. 11, pp. 4405–4417, 2015.

[18] J. Xu, Z. Zhong, and B. Ai, "Wireless powered sensor networks: Collaborative energy beamforming considering sensing and circuit power consumption," *IEEE Wireless Communications Letters*, vol. 5, no. 4, pp. 344–347, 2016.

[19] N. K. D. Venkategowda, H. Lee, and I. Lee, "Data precoding and energy transmission for parameter estimation in MIMO wireless powered sensor networks," in *2017 IEEE 86th Vehicular Technology Conference (VTC-Fall)*, 2017, pp. 1–5.

[20] ——, "Joint transceiver designs for MSE minimization in MIMO wireless powered sensor networks," *IEEE Transactions on Wireless Communications*, vol. 17, no. 8, pp. 5120–5131, 2018.

[21] S. Knorn, S. Dey, A. Ahlén, and D. E. Quevedo, "Distortion minimization in multi-sensor estimation using energy harvesting and energy sharing," *IEEE Transactions on Signal Processing*, vol. 63, no. 11, pp. 2848–2863, 2015.

[22] S. Knorn, S. Dey, A. Ahlén, and D. E. Quevedo, "Optimal energy allocation in multisensor estimation over wireless channels using energy harvesting and sharing," *IEEE Transactions on Automatic Control*, vol. 64, no. 10, pp. 4337–4344, 2019.

[23] P. Wu, F. Xiao, C. Sha, H. Huang, and L. Sun, "Trajectory optimization for UAVs' efficient charging in wireless rechargeable sensor networks," *IEEE Transactions on Vehicular Technology*, vol. 69, no. 4, pp. 4207–4220, 2020.

[24] Y. Liu, Q. Shi, Q. Wu, J. Zhao, and M. Li, "Joint node activation, beamforming and phase-shifting control in IoT sensor network assisted by reconfigurable intelligent surface," *IEEE Transactions on Wireless Communications*, vol. 21, no. 11, pp. 9325–9340, 2022.

[25] M. F. Ahmed, K. P. Rajput, N. K. D. Venkategowda, K. V. Mishra, and A. K. Jagannatham, "Joint transmit and reflective beamformer design for secure estimation in IRS-aided WSNs," *IEEE Signal Processing Letters*, vol. 29, pp. 692–696, 2022.

[26] Z. Chu, Z. Zhu, F. Zhou, M. Zhang, and N. Al-Dhahir, "Intelligent reflecting surface assisted wireless powered sensor networks for internet of things," *IEEE Transactions on Communications*, vol. 69, no. 7, pp. 4877–4889, 2021.

[27] W. Du, Z. Chu, G. Chen, P. Xiao, Y. Xiao, X. Wu, and W. Hao, "STAR-RIS assisted wireless powered IoT networks," *IEEE Transactions on Vehicular Technology*, pp. 1–15, 2023.
[28] Z. Wang, Y. Shi, Y. Zhou, H. Zhou, and N. Zhang, "Wireless-powered over-the-air computation in intelligent reflecting surface-aided IoT networks," *IEEE Internet of Things Journal*, vol. 8, no. 3, pp. 1585–1598, 2021.
[29] S. Dinh-Van, T. M. Hoang, R. Trestian, and H. X. Nguyen, "Unsupervised deep-learning-based reconfigurable intelligent surface-aided broadcasting communications in industrial IoTs," *IEEE Internet of Things Journal*, vol. 9, no. 19, pp. 19 515–19 528, 2022.
[30] X. Cheng, P. Khanduri, B. Chen, and P. K. Varshney, "Joint collaboration and compression design for distributed sequential estimation in a wireless sensor network," *IEEE Transactions on Signal Processing*, vol. 69, pp. 5448–5462, 2021.
[31] X. Cheng, B. Geng, P. Khanduri, B. Chen, and P. K. Varshney, "Joint collaboration and compression design for random signal detection in wireless sensor networks," *IEEE Signal Processing Letters*, vol. 28, pp. 1630–1634, 2021.
[32] Z. Fang, J. Wang, Y. Ren, Z. Han, H. V. Poor, and L. Hanzo, "Age of information in energy harvesting aided massive multiple access networks," *IEEE Journal on Selected Areas in Communications*, vol. 40, no. 5, pp. 1441–1456, 2022.
[33] C. Battiloro, P. Di Lorenzo, P. Banelli, and S. Barbarossa, "Dynamic resource optimization for decentralized estimation in energy harvesting IoT networks," *IEEE Internet of Things Journal*, vol. 8, no. 10, pp. 8530–8542, 2021.
[34] C. Zhan, Y. Zeng, and R. Zhang, "Trajectory design for distributed estimation in UAV-enabled wireless sensor network," *IEEE Transactions on Vehicular Technology*, vol. 67, no. 10, pp. 10 155–10 159, 2018.
[35] S. Biswas, S. Dey, S. Knorn, and A. Ahlén, "On optimal quantized non-Bayesian quickest change detection with energy harvesting," *IEEE Transactions on Green Communications and Networking*, vol. 4, no. 2, pp. 433–447, 2020.
[36] A. Sani and A. Vosoughi, "Distributed vector estimation for power- and bandwidth-constrained wireless sensor networks," *IEEE Transactions on Signal Processing*, vol. 64, no. 15, pp. 3879–3894, 2016.
[37] ——, "On distributed linear estimation with observation model uncertainties," *IEEE Transactions on Signal Processing*, vol. 66, no. 12, pp. 3212–3227, 2018.
[38] I. Nevat, G. W. Peters, and I. B. Collings, "Random field reconstruction with quantization in wireless sensor networks," *IEEE Transactions on Signal Processing*, vol. 61, no. 23, pp. 6020–6033, 2013.
[39] H. Leung, C. Seneviratne, and M. Xu, "A novel statistical model for distributed estimation in wireless sensor networks," *IEEE Transactions on Signal Processing*, vol. 63, no. 12, pp. 3154–3164, 2015.
[40] D. Ciuonzo, S. H. Javadi, A. Mohammadi, and P. S. Rossi, "Bandwidth-constrained decentralized detection of an unknown vector signal via multisensor fusion," *IEEE Transactions on Signal and Information Processing over Networks*, vol. 6, pp. 744–758, 2020.
[41] K. P. Rajput, M. F. Ahmed, N. K. D. Venkategowda, A. K. Jagannatham, G. Sharma, and L. Hanzo, "Robust decentralized and distributed estimation of a correlated parameter vector in MIMO-OFDM wireless sensor networks," *IEEE Transactions on Communications*, vol. 69, no. 10, pp. 6894–6908, 2021.
[42] N. K. Venkategowda, B. B. Narayana, and A. K. Jagannatham, "Precoding for robust decentralized estimation in coherent-MAC-based wireless sensor networks," *IEEE Signal Processing Letters*, vol. 24, no. 2, pp. 240–244, 2017.
[43] J. Zhu, R. S. Blum, X. Lin, and Y. Gu, "Robust transmit beamforming for parameter estimation using distributed sensors," *IEEE Communications Letters*, vol. 20, no. 7, pp. 1329–1332, July 2016.
[44] Y. Liu, J. Li, and H. Wang, "Robust linear beamforming in wireless sensor networks," *IEEE Transactions on Communications*, vol. 67, no. 6, pp. 4450–4463, 2019.
[45] K. P. Rajput, A. Kumar, S. Srivastava, A. K. Jagannatham, and L. Hanzo, "Bayesian learning-based linear decentralized sparse parameter estimation in MIMO wireless sensor networks relying on imperfect CSI," *IEEE Transactions on Communications*, vol. 69, no. 9, pp. 6236–6250, 2021.
[46] K. P. Rajput, Y. Verma, N. K. D. Venkategowda, A. K. Jagannatham, and P. K. Varshney, "Robust linear transceiver designs for vector parameter estimation in MIMO wireless sensor networks under csi uncertainty," *IEEE Transactions on Vehicular Technology*, vol. 70, no. 8, pp. 7347–7362, 2021.
[47] P. Ubaidulla and A. Chockalingam, "Relay precoder optimization in MIMO-relay networks with imperfect CSI," *IEEE Transactions on Signal Processing*, vol. 59, no. 11, pp. 5473–5484, 2011.
[48] Y. Guo and B. C. Levy, "Worst-case MSE precoder design for imperfectly known MIMO communications channels," *IEEE Transactions on Signal Processing*, vol. 53, no. 8, pp. 2918–2930, Aug 2005.
[49] J. Li and G. AlRegib, "Rate-constrained distributed estimation in wireless sensor networks," *IEEE Transactions on Signal Processing*, vol. 55, no. 5, pp. 1634–1643, May 2007.
[50] B. Widrow, I. Kollar, and Ming-Chang Liu, "Statistical theory of quantization," *IEEE Transactions on Instrumentation and Measurement*, vol. 45, no. 2, pp. 353–361, April 1996.
[51] S. Boyd and L. Vandenberghe, *Convex optimization*. Cambridge university press, 2004.
[52] K. B. Petersen and M. S. Pedersen, "The matrix cookbook," Nov. 2012, version 20121115. [Online]. Available: http://www2.compute.dtu.dk/pubdb/pubs/3274-full.html
[53] Y. Ye, *Interior point algorithms: theory and analysis*. Springer, 1997.
[54] E. A. Gharavol and E. G. Larsson, "The sign-definiteness lemma and its applications to robust transceiver optimization for multiuser MIMO systems," *IEEE Transactions on Signal Processing*, vol. 61, no. 2, pp. 238–252, 2013.